HYDROTHERMAL METHOD FOR DOPING OF ZINC OXIDE NANOWIRES AND FABRICATION OF ULTRAVIOLET PHOTODETECTORS

A THESIS SUBMITTED TO
THE GRADUATE SCHOOL OF NATURAL AND APPLIED SCIENCES
OF
MIDDLE EAST TECHNICAL UNIVERSITY

BY

AYŞEGÜL AFAL

IN PARTIAL FULFILLMENT OF THE REQUIREMENTS
FOR
THE DEGREE OF MASTER OF SCIENCE
IN
METALLURGICAL AND MATERIALS ENGINEERING

JULY 2012

Approval of the thesis:

HYDROTHERMAL METHOD FOR DOPING OF ZINC OXIDE NANOWIRES AND FABRICATION OF ULTRAVIOLET PHOTODETECTORS

submitted by **AYŞEGÜL AFAL** in partial fulfillment of the requirements for the degree of **Master of Science in Metallurgical and Materials Engineering Department, Middle East Technical University** by,

Prof. Dr. Canan ÖZGEN _____
Dean, Graduate School of **Natural and Applied Sciences**

Prof. Dr. C. Hakan GÜR _____
Head of Department, **Metallurgical and Materials Engineering**

Assist. Prof. Dr. Hüsnü Emrah ÜNALAN _____
Supervisor, **Metallurgical and Materials Eng. Dept., METU**

Prof. Dr. Raşit TURAN
Co-Supervisor, **Physics Dept., METU** _____

Examining Committee Members:

Prof. Dr. Tayfur ÖZTÜRK _____
Department of Metallurgical and Materials Engineering, METU

Assist. Prof. Dr. Hüsnü Emrah ÜNALAN _____
Department of Metallurgical and Materials Engineering, METU

Assoc. Prof. Dr. Caner DURUCAN _____
Department of Metallurgical and Materials Engineering, METU

Assist. Prof. Dr. Yunus Eren KALAY _____
Department of Metallurgical and Materials Engineering, METU

Assist. Prof. Dr. Alpan BEK _____
Department of Physics, METU

Date: *06.07.2012*

I hereby declare that all information in this document has been obtained and presented in accordance with academic rules and ethical conduct. I also declare that, as required by these rules and conduct, I have fully cited and referenced all material and results that are not original to this work.

Name, Last name: Ayşegül AFAL
Signature :

ABSTRACT

HYDROTHERMAL METHOD FOR DOPING OF ZINC OXIDE NANOWIRES AND FABRICATION OF ULTRAVIOLET PHOTODETECTORS

AFAL, Ayşegül
M. Sc., Department of Metallurgical and Materials Engineering
Supervisor: Assist. Prof. Dr. Hüsnü Emrah ÜNALAN
Co-Supervisor: Prof. Dr. Raşit TURAN

July 2012, 75 pages

Nanotechnology comprises of the understanding and control of materials and processes at the nanoscale. Among various nanostructured materials, semiconducting nanowires attract much interest for their novel physical properties and potential device applications. The unique properties of these nanowires are based on their high surface to volume ratio and quantum confinement effect.

Zinc oxide, having a direct, wide bandgap and large exciton binding energy, is highly appealing for optoelectronic devices. Due to excellent optical and electrical properties, zinc oxide nanowires have been utilized to fabricate various devices such as solar cells, light emitting diodes, transistors and photodetectors. Furthermore, zinc oxide, in its natural state exhibits n-type conductivity. Addition of impurities often

leads to remarkable changes in their electrical and optical properties, which open up new application areas.

Among the many synthesis methods for zinc oxide nanowires, hydrothermal method is an attractive one due to its easy procedure, simple equipment and low temperature requirements.

In this thesis, zinc oxide nanowires were grown and doped by hydrothermal method. Different metal dopants such as copper, silver and aluminum were used for this purpose. These metals were selected as dopants due to their effect on magnetic properties, p-type conduction and electrical conductivity of ZnO nanowires, respectively. Doped nanowires were fully characterized and the changes in their physical properties were investigated.

In addition, hydrothermally synthesized pure and aluminum doped zinc oxide nanowires were used as the electrically active components in ultraviolet photodetectors. Silver nanowires were utilized as transparent electrodes. Optoelectronic properties of the detectors were examined. Effect of in-situ annealing and nanowire length was investigated. Short recovery time, around 4 seconds, with a decent on/off ratio of 2600 was obtained. This design provides a simple and cost effective approach for the fabrication of high performance ultraviolet photodetectors.

Keywords: zinc oxide nanowires, doping, ultraviolet photodetectors

ÖZ

ÇİNKO OKSİT NANOTELLERİN HİDROTERMAL YÖNTEMLE AŞILANMASI VE ULTRAVIYOLE FOTODEDEKTÖR ÜRETİMİ

AFAL, Ayşegül
Yüksek Lisans, Metalurji ve Malzeme Mühendisliği Bölümü
Tez Yöneticisi: Yrd. Doç. Dr. Hüsnü Emrah ÜNALAN
Ortak Tez Yöneticisi: Prof. Dr. Raşit TURAN

Temmuz 2012, 75 sayfa

Nanoteknoloji, nanoboyuttaki malzemelerin ve proseslerin kavranması ve kontrolünü kapsamaktadır. Çeşitli nanoyapılı malzemeler arasında, yarıiletken nanoteller özgün fiziksel özellikleri ve potansiyel cihaz uygulamaları açısından fazlaca ilgi çekmektedirler. Nanotellerin eşsiz özellikleri, sahip oldukları yüksek yüzey-hacim oranlarına ve kuantum sınırlamasına dayanır.

Doğrudan geniş bant aralığı ve yüksek elektron-hol bağlama enerjisine sahip olan çinko oksit, optoelektronik cihazlar için oldukça cazip bir malzemedir. Üstün optik ve elektriksel özellikleri sebebiyle, çinko oksit nanoteller güneş pilleri, ışık yayan diyotlar, transistörler ve fotodedektörler gibi çeşitli cihazların üretiminde kullanılmıştır. Ayrıca, çinko oksit doğal olarak n-tipi iletkenlik göstermektedir. Yapıya eklenen katışkıların nanotellerin elektriksel ve optik özelliklerinde değişime yol açması, yeni uygulama alanları yaratmaktadır.

Birçok çinko oksit nanotel sentezleme yöntemi arasında hidrotermal yöntem kolay uygulanması, basit ekipman ve düşük sıcaklık gereksinimleriyle cazip bir metottur.

Bu tez çalışmasında, çinko oksit nanoteller hidrotermal yöntemle büyütülmüş ve aşılanmıştır. Aşılama için, bakır, gümüş ve alüminyum gibi farklı metal katkılayıcılar kullanılmıştır. Bu metaller sırasıyla çinko oksit nanotellerin manyetik özellikleri, p-tipi iletim ve elektriksel iletkenliğine etkileri sebebiyle seçilmiştir. Aşılanmış nanoteller bütünüyle karakterize edilmiştir ve fiziksel özelliklerindeki değişimler araştırılmıştır.

Ayrıca, hidrotermal yöntemle sentezlenmiş katkısız ve alüminyum katkılı çinko oksit nanoteller ultraviyole fotodedektörlerde elektriksel aktif bileşen olarak kullanılmıştır. Transparan elektrot olarak gümüş nanoteller kullanılmıştır. Dedektörlerin optoelektronik özellikleri incelenmiştir. Yerinde tavlama ve nanotel boyunun dedektör üzerindeki etkileri araştırılmıştır. Yaklaşık 4 saniye gibi düşük bir akım azalma süresi ve 2600 gibi makul bir açma-kapama oranı elde edilmiştir. Bu dizayn yüksek performanslı ultraviyole fotodedektörlerin üretimi için kolay ve uygun maliyetli bir yaklaşım sağlamaktadır.

Anahtar Kelimeler: çinko oksit nanoteller, aşılama, ultraviyole fotodedektörler

To My Family…

ACKNOWLEDGEMENTS

I would like to thank my advisor Assist. Prof. Dr. Emrah Ünalan for his support and guidence throughout the whole time I have worked on this project and Prof. Dr. Raşit Turan for giving me the opportunity to occupy all the facilities in the Physics Dept. and his support for my studies. In addition, I would like to thank to Prof. Dr. Mehmet Parlak for his guidance throughout all the experiments. I also would like to thank Prof. Dr. Ekmel Özbay, Pakize Demirel, Ayça Emen and Deniz Çalışkan for their help in optical and electrical measurements.

I also would like to thank Necmi Avcı, Saffet Ayık, Serkan Yılmaz and Assist. Prof. Dr. Eren Kalay for spending infinite hours of SEM and XRD sessions.

I wish to give my special thanks to my friend of long years, Başak Aysin, for her support from the beginning to the end. METU and METE would be very different without you. I also wish to thank to Aybüge Çekinmez for being such a good friend and for providing me a great deal of support.

I owe my deepest gratitude to my lab-mates and dearest friends Barış Özdemir, Elif Selen Ateş, Burcu Aksoy, Şeyda Küçükyıldız and Emre Mülazımoğlu for their infinite support, patience and kindness. I will never forget the awesome time we have had together and I feel very lucky to get to know such great people. I feel the need to single out Mustafa Kulakcı and Şahin Coşkun, for their guidance and patience and never fed up to help me when I' m stuck. I would not have been able to accomplish this task without their invaluable contributions. I also appreciate the great moral support from Güher Kotan, Evren Tan, Can Yıldırım, Halil İbrahim Yavuz, Mehmet Can Akgün, Fırat Es, Olgu Demircioğlu and all my friends who have helped and supported me all along.

And finally, I would like to thank my parents for their patience along my studies. My special thanks go to Evren Geniş...I cannot describe my feelings with any words, your love is the most valuable thing I have... Thank you for everything, thank you for always being there for me.

TABLE OF CONTENTS

LIST OF TABLES

TABLES

LIST OF FIGURES

FIGURES

CHAPTER 1

INTRODUCTION

The advancements in technology has brought new materials and innovative devices particularly in the field of electronics. In today's world, nanotechnology becomes one of the most popular technologies being used to fabricate different devices for various applications. Basically, this new technology includes the design, fabrication, characterization and application of nanomaterials. Nanotechnology deals with the molecular and atomic levels of ultra small structures, at a length scale of 1-100 nm. Properties and functions of devices and systems vary with a decrease in their size and the field of nanotechnology deals with either understanding their nature or creating new materials.

Semiconductor materials, which act as the basic building blocks in electronics, can be a part of nanotechnology field due to the possibility of miniaturization of the devices. In addition, doping of these semiconductors leads to remarkable changes in their physical properties such as type of majority carriers, electrical conductivity, optical properties, bandgap and magnetic properties [1].

The last decades have witnessed considerable development in the synthesis, characterization and applications of nanomaterials. Among nanostructured materials, one-dimensional types have constantly been subjected to intense attention due to their high aspect ratio dependent, unique physical and chemical properties. Since nanowires, as an important one-dimensional material, can be in either metallic or semiconducting nature, they are used in various applications. Having a direct wide band-gap (3.37 eV) and high exciton binding energy (60 meV), inherently n-type

semiconducting ZnO is a significant material for optoelectronic applications. Single crystalline and almost defect free nature with a high surface to volume ratio, nanostructures of ZnO also received intense attention. Among ZnO nanostructures, nanowires/nanorods have been proved to be used as active materials in ultraviolet (UV) lasers [2], solar cells [3], nano-generators [4], transistors [5] and photodetectors [6].

ZnO is naturally an n-type semiconductor and n or p-type behavior can be controlled by the addition of different dopant metals. As in the case of most oxide materials, n-type doping of ZnO is straightforward but it is difficult to dope it p-type. It is highly attractive to obtain reproducible and stable p-type doped ZnO for the fabrication of homojunction optoelectronic devices and this area still remains challenging and debatable.

Another important research topic is the detection of UV radiation, which in excess inversely affects human life. The most important UV source is the sun. The UV radiation includes UVA, UVB, UVC and the far UV. It is known that UVA and UVB are responsible for the biological effects of the sun. UV photodetection is also important for the use in military and medical applications. For most of the applications, it is advantageous if the UV photodetectors are not sensitive to visible and infrared radiation. Therefore, they are classified as visible blind detectors with cutoff wavelengths in between 280-400 nm, also named as solar blind presuming that the UVC can be blocked by the atmosphere. In addition, a suitable UV photodetector should meet the necessary requirements such as high sensitivity in UV region, low signal to noise ratio, high selectivity and responsivity.

ZnO will also be a convenient candidate for UV photodetection with its direct wide bandgap. Many researchers have reported UV photodetectors utilizing ZnO nanowires. However, high vacuum and high temperature processes such as chemical vapor deposition, thermal evaporation and sputtering were used to fabricate most of these aforementioned photodetectors. Hydrothermally grown ZnO nanowires can be used as the active material in UV photodetectors to achieve low cost fabrication.

Generally, non-transparent metal electrodes are used in ZnO UV photodetectors. Nevertheless, these electrodes lead to a decrease in the amount of absorbed light and are deposited through high vacuum processes. Among the alternative transparent and conducting contacts, random networks of silver (Ag) nanowires can be promising candidates.

In this thesis, ZnO nanowire synthesis methods were explained and hydrothermal ZnO nanowire growth was investigated in Chapter 2. Then, in Chapter 3, hydrothermal method was used to dope the ZnO nanowires. Copper, silver and aluminum were used as dopant elements to impart and consequently examine the magnetic properties, p-type doping and enhanced conductivity, respectively. Finally in Chapter 4, all solution based UV photodetectors utilizing ZnO and Ag nanowires were developed. Structural and optoelectronic properties of these UV photodetectors fabricated on glass substrates were investigated in detail.

CHAPTER 2

ZINC OXIDE NANOWIRE SYNTHESIS BY HYDROTHERMAL METHOD

2.1 Introduction

In recent years, ZnO has attracted great attention with its significant piezoelectric and semiconducting properties. This interest owes much of its importance to the use of ZnO in optoelectronic applications.

Although ZnO has been extensively studied for years, detailed investigation of its novel semiconducting properties has begun in the mid- to late 1950's. In 1960's, extensive studies such as band structure, excitonic and electrical transport properties of intrinsic ZnO were carried out. Quite recently, it was found that ZnO can be a good competitor to gallium nitride (GaN) due to their similarities in bandgap and lattice parameters [7]. In addition, ZnO has a larger exciton binding energy (~ 60 meV as opposed to 25 meV for GaN), abundant and can be produced through simpler and cost-effective crystal growth methods compared to GaN.

In the past decade, various studies have been carried out on both fabrication and application of nanostructured ZnO. ZnO nanomaterials are highly appealing candidates for photonics and nanoelectronic devices due to their superior properties.

2.1.1 Zinc Oxide

ZnO, as a group II-VI compound semiconductor, has a direct wide bandgap (3.37 eV). The three different crystal structures of ZnO are i) rocksalt, ii) zinc blende and iii) hexagonal wurtzite. They are schematically shown in Figure 2.1.

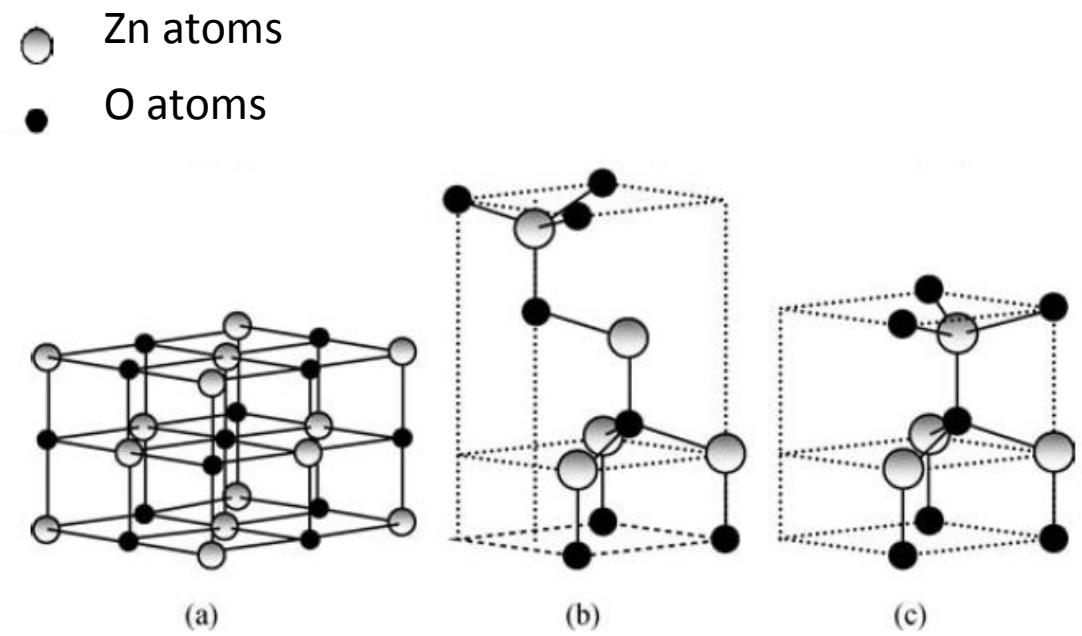

Figure 2.1 Different ZnO crystal structures: a) rocksalt, b) zinc blende and c) hexagonal wurtzite [8].

At ambient conditions, ZnO has wurtzite structure due to its thermodynamic stability. Ideally, this wurtzite ZnO unit cell is hexagonal and has two lattice parameters with the ratio of c/a=1.633 and the structure's space group is $P6_3mc$ [8]. Generally, the electrical properties of ZnO are related to the crystal defects in its structure. ZnO is an unintentionally doped n-type semiconductor due to naturally occurring oxygen vacancies.

ZnO is used in optoelectronic and microelectronic devices in the form of bulk crystals, epitaxial thin film layers and nanostructures [9]. High quality ZnO bulk

crystals as large size substrates are significant for both material science and many device applications [8]. However, due to high prices of bulk ZnO, epitaxial ZnO thin films provide a better alternative due to their low deposition temperature, transparency in visible region and decent electrical conductivity [10].

In recent years, ZnO nanomaterials with reduced dimensions and novel properties became the center of attention for nanoelectronic device applications due to the simple and cost-effective crystal growth methods. Among ZnO nanostructures, nanowires and nanorods are one of the most attractive candidates to investigate the dependence of thermal, mechanical and electrical properties on dimensionality and size reduction.

2.1.2 General Characteristics of Nanowires

Nanostructured polycrystalline materials have a modest size of grains with only several hundreds of atoms; whereas, bulk material grains may differ from several microns to mm in size that has been formed up of billions of atoms. As the grain size -and inevitably, the number of atoms- decrease in a drastic fashion, the density of the grain boundaries and interfaces increase substantially. Since the chemical potential is higher at the surface in contrast to the bulk region, nanostructured materials have intensified optical, mechanical, magnetic and electrical properties in comparison to the bulk materials.

Taking various methods of synthesis into consideration, nanostructured materials can be classified according to their dimensions as presented in Figure 2.2.

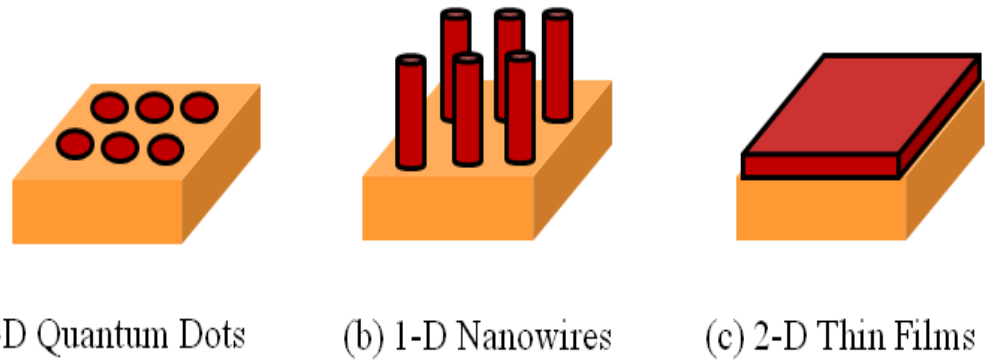

Figure 2.2 Schematics of nanostructured materials in terms of their dimensions.

Nanowire is a one dimensional system, with two quantum confined directions, and one unconfined direction in order to conduct electrons through. Advanced state of electrical and optical properties of nanomaterials is based on the quantum confinement effect. Quantum confinement is the trapping of charge carriers in an area small enough that their quantum (wave-like) behavior dominates over their classical (particle-like) behavior. In terms of quantum mechanics, the requirement for quantum confinement is that the dimension of the confining device or particle must be equal to, or smaller than, the de Broglie wavelength of the carriers, the carrier inelastic mean free path and electron-hole Bohr radius of the used material. Depending on their unique density of electronic states, nanowires with sufficiently small diameters are expected to present considerably different electrical, optical and magnetic properties from their bulk counterparts. In addition, nanowires differ from bulk materials in terms of their single crystalline and grain boundary free nature, the increased surface area to volume ratio, very high density of electronic states, enhanced exciton binding energy, diameter-dependent bandgap and increased surface scattering for electrons and phonons [11].

2.1.3 Applications of ZnO Nanowires

Nanowires are appealing for optoelectronic applications due to their small size and low power consumption. ZnO nanowires have been already utilized as active components in field effect transistors (FETs) [12,13], light emitting diodes (LEDs) [14], gas sensors [15], ultraviolet (UV) photodetectors [16] and solar cells [17].

Depending on their novel electrical properties, one of the leading research topics in nanoelectronics is the utilization of ZnO nanowires in FETs. FETs are common parts of the most electronic devices. Their operation principle is based on the diffusion of one type of charge carrier by the application of a voltage to the gate electrode to create a conducting channel between source and drain electrodes. Owing to the single crystalline structure of ZnO nanowires, nanowire based FETs demonstrate high carrier mobility compared to organic, amorphous silicon thin film and polycrystalline silicon transistors [6]. Various research groups have studied the electrical properties of ZnO nanowire based FETs. For example, Cha et. al. fabricated single ZnO nanowire FET devices and characterized their transport properties. Their study revealed that; these n-type nanowire transistors have excellent performance with a transconductance of 3.06 μS, a field effect mobility of 928 cm^2/ V.s, and an on/off current ratio of 10^6 [13].

Fabrication of LEDs with ZnO nanowires as the active component is also an attractive application field. LED is a device that consists of negatively and positively charged semiconductors creating a p-n junction. ZnO, as an n-type semiconductor, is a convenient material for blue or UV LEDs due to its wide bandgap. ZnO nanowires with their high surface to volume ratio can be used as negatively charged semiconducting part of the heterojunction LEDs. The utilization of single crystalline ZnO nanowires in LEDs also eliminates the problems with the grain boundaries. In addition, the reduced contact area between n and p-type semiconductors results in high quality junctions with low defect density and interfacial strain [14]. Generally, GaN thin films are used to fabricate blue and UV LEDs. ZnO, as an alternative material for the fabrication of UV LEDs, has the same crystal and band structure with GaN with larger exciton binding energy. Furthermore, ZnO nanowires are abundantly available and less expensive to grow compared with GaN [18].

Another promising approach can be the fabrication of ZnO nanowire homojunction LEDs. These homojunctions comprise n and p-type ZnO nanowire layers acting as electron and hole injection layers, respectively. However, it is difficult to synthesize low resistivity and stable p-type ZnO nanowires due to the self-compensation mechanism related to oxygen vacancies and zinc interstitials and the low solubility of dopants [19]. On the other hand, various studies are available concerning the fabrication of homojunction LEDs in which p-type doping was achieved by ion implantation [20], thermal diffusion [21] and hydrothermal processes [22].

ZnO nanowires can also be used for gas sensing applications. Gas sensors are devices, which convert the physical characteristic of a gas into electronic signals. The working principle of ZnO based gas sensors depend on the chemisorption of oxygen onto their surface. Following the charge transfer due to the reaction between the chemisorbed oxygen and target gases, the surface resistance of the sensor material changes [23]. Due to high chemical stability, sensitivity to various adsorbed gases, large surface to volume ratio and non-toxicity, ZnO nanowires were identified as convenient materials for the fabrication of gas sensors [15].

Another interesting characteristic of ZnO nanowires is the UV detection properties. Due to nanowires' high surface to volume ratio and large number of surface traps, the photogenerated carrier lifetime increases. Furthermore, reduced dimensions cause a decrease in the carrier transit time [16]. In a related study, Kind et. al. revealed the possibility of fabricating nanowire based switches using the photoconductivity of individual semiconductor ZnO nanowires [24].

Utilization of ZnO nanowires in solar cells has also become an appealing research field in the past few decades. Solar cells are the devices that convert solar power into electricity. Among different solar cell types, dye sensitized solar cells (DSSC) can be fabricated using ZnO nanowires. For these solar cells, improved electron transport and high surface area for dye adsorption are important parameters. ZnO nanowires can provide both direct conduction path for electrons and required high surface area [25]. In addition, they have low reflectivity, which enhances light absorption. Law et. al. presented a study on ZnO nanowire based DSSCs. In this study, they introduced a version of DSSC, in which instead of traditional nanoparticle films, solution grown

ZnO nanowires were used as the direct electrical pathways. Furthermore, use of nanowires resulted in the rapid collection of carriers generated throughout the cell [17]. Schematic of various devices utilizing ZnO nanowires are provided in Figure 2.3. As indicated before, nanowires impart remarkable characteristics to the most of these optoelectronic devices.

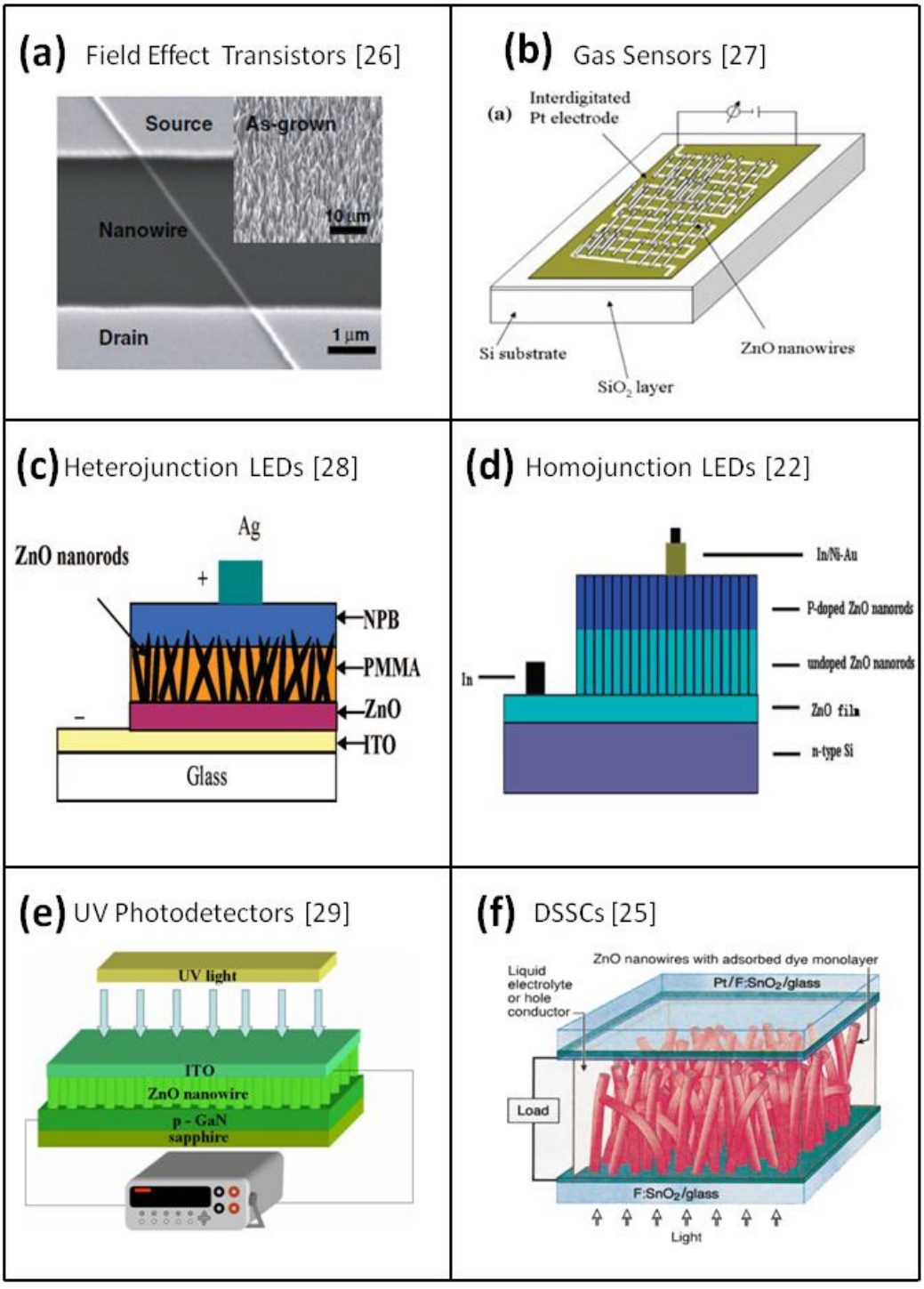

Figure 2.3 Schematic of various devices utilizing ZnO nanowires.

2.1.4 Conventional Zinc Oxide Nanowire Synthesis Methods

Nanowire synthesis methods similar to other nanomaterials are generally based on two approaches, namely bottom-up and top-down strategies. The top down approach include etching of bulk materials to form the required structure. On the other hand, in the bottom-up approach, nanowires are formed from their building blocks. In accordance with these approaches, ZnO nanowires are commonly synthesized using one of the following two general mechanisms, namely, vapor phase and solution based growth.

2.1.4.1 Top-Down Based Synthesis

Template assisted growth, as a top-down approach, can also be used for ZnO nanowire synthesis. Well aligned ZnO nanowires on various substrates can be synthesized through this method. The mechanical properties and the chemical stability of the template, as well as the density, diameter and uniformity of its pores are important parameters. The most commonly used template for ZnO nanowire growth includes anodic alumina membranes [30]. Lithography is the most commonly used method for the fabrication of templates. The aligned ZnO nanowires increase the quality of the fabricated devices. Nevertheless, top-down approaches have less reproducibility and controllability compared with other techniques.

2.1.4.2 Vapor Phase Growth

Vapor phase growth is divided into two categories, which are vapor-liquid-solid (VLS) and vapor-solid (VS) approaches. During VLS process, the growth mechanism involves the absorption of source material from the gas phase into a liquid droplet of metal catalyst. In case of ZnO nanowire growth, the commonly used metal catalyst is gold (Au) [31]. The liquid droplet initially acts as appropriate site for gas phase reactant absorption and after supersaturation of this liquid alloy, nucleation site forms for crystallization. The catalyst droplet affects the growth

direction and controls the nanowire diameter. The growth ends when no reactant remains in the system or the ambient temperature decreases under the eutectic temperature of the catalyst alloy. A nanowire that has been grown via VLS mechanism generally has a metal nanoparticle located at its tip [32]. The VLS growth mechanism is schematically shown in Figure 2.4.

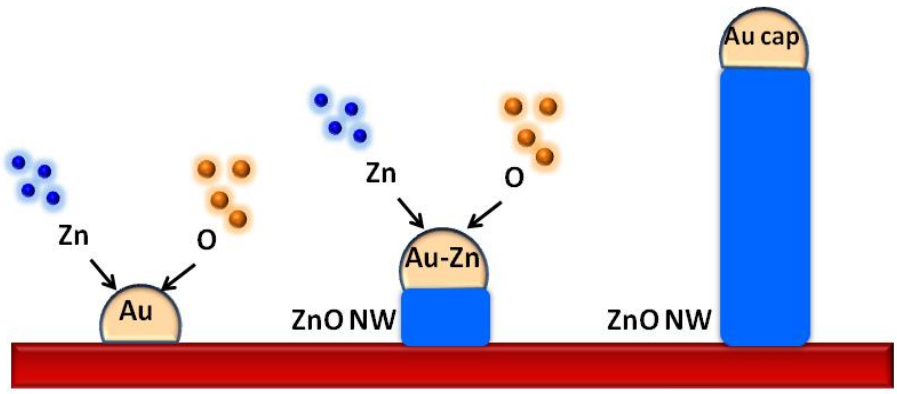

Figure 2.4 Schematic of the stages of VLS growth mechanism for ZnO nanowires.

On the other hand, in the VS process, instead of using a metal catalyst, the gas phase reactants nucleate directly on the seed layer composed of ZnO under controlled temperature and pressure. This approach is preferred for device applications, because of the absence of metal particles at the tip of the nanowires. Various nanostructured materials can be synthesized using this method. However, by VS process, the control of alignment, geometry and accurate location of ZnO nanowires become difficult.

Commonly used vapor deposition techniques for the growth of ZnO nanowires include physical vapor deposition (PVD) [33], chemical vapor deposition (CVD) [34] and metal organic chemical vapor deposition (MOCVD) [35]. Basically, a vacuum system and a reactor through which the precursor gas flows are employed in these methods. In CVD method, the precursor chemicals decompose or react on the substrate surface and the resulting reaction forms the nanowires. MOCVD differs from CVD in terms of used organic compounds. In PVD, the precursor is heated till

sublimation, which then meets the cold substrate and condenses. In addition, pulsed laser deposition and thermal evaporation are two different PVD methods.

2.1.4.3 Solution Based Growth

The other general method for ZnO nanowire synthesis is solution based. Compared to vapor phase methods, solution based methods can be scaled up for large area applications. The lower growth temperatures and cost effectiveness of this method are appealing for scientists and industry. Electrochemical deposition and hydrothermal method can be revealed as two different routes for this growth technique. Electrochemical deposition is a convenient technique to form uniform ZnO nanowires over large areas through the application of an external driving force for reactions. Nanowires can be grown on conducting substrates without using seeds. In a classical electrochemical deposition experiment, precursor chemicals are dissolved generally in deionized (DI) water and the solution is kept on a hot plate at the desired temperature. In addition, a reference electrode made of a platinum wire and a power source to apply potential difference between the substrate and electrode is used. Zinc chloride and potassium chloride are used as electrolytes [36]. However, this method is more complex and needs an external power supply compared to the hydrothermal growth.

Hydrothermal growth, on the other hand, is a very powerful and versatile technique for nanowire growth. Generally, this method includes chemical reactions in aqueous solutions. These reactions can be considered to be in reversible equilibrium and the driving force is the minimization of the free energy of the whole reaction system. ZnO nanowires with wurtzite crystal structure are grown along their c-axis, which is a high energy polar surface, such as ± (0001) with alternating O^{2-} terminated and Zn^{2+} terminated surfaces. During the nanowire formation, due to the high energy of the polar surfaces, the precursor molecules tend to get adsorbed on these surfaces. After the adsorption of the precursor molecules to the surface, another polar surface is formed with inverted polarity. For example, a Zn^{2+} terminated surface becomes an O^{2-} terminated surface. This process is repeated over time and leads to the growth of

nanowires along the ± [0001] directions. The non-polar {2-1-10} and {1-100} side surfaces are exposed to the solution [37]. The various crystal morphologies of ZnO depend on the surface energy differences of crystal faces and external growth environment.

Growth of highly oriented ZnO nanowires using hydrothermal method has been studied by various scholars. Andrés-Vergés et. al. [38] initiated the aqueous solution synthesis for the first time and then it was developed further by Vayssieres et. al. [39] to grow directly onto a substrate. Generally, a ZnO seed layer is used to initialize uniform nanowire growth. This seed layer can be obtained in different ways such as, sputtering of ZnO thin films or spin coating of zinc acetate solution to form ZnO crystallites by heat treatment [40].

Great effort has been spent to understand the mechanism of the hydrothermal synthesis of ZnO nanowires, since it is the simplest, most appealing and low cost method among the other methods mentioned earlier. In addition, using this method, ZnO nanowires can be grown over large areas and on any type of substrate including plastics, which do not tolerate high temperatures.

Hydrothermal growth parameters used in this thesis are explained below.

2.2 Experimental Details

In order to obtain high quality well-aligned nanowires, the substrate surfaces must be completely free of contaminants. Any contaminated area may cause disrupted structure or hinder nanowire formation. Therefore, all type of substrates including silicon (Si) wafer, soda-lime silica glass and indium tin oxide (ITO) coated glass were cleaned with acetone (99.8% pure), isopropanol (99.8% pure) and DI water in an ultrasonic bath for 10 minutes each. Then, the substrates were dried under nitrogen flow. All chemicals were purchased from Sigma-Aldrich and used without further purification.

Hydrothermal growth of ZnO nanowires on substrates starts with the deposition of the seed layer which is followed by the growth of nanowires within a solution.

Initially, ZnO seed layer was deposited through spin coating a 5 mM zinc acetate dihydrate solution in 1-propanol. This solution was typically spin coated at 2000 rpm for 1 minute. Zinc acetate coated substrates were annealed at 120°C on a hot plate for drying. This procedure can be carried out a number of times depending on the required density of seeds and ultimately nanowires. Then, seeded substrates were immersed into an equimolar (20 mM) aqueous solution of zinc acetate dihydrate ($Zn(O_2CCH_3)_2(H_2O)_2$) and hexamethylenetetramine (HMTA) in DI water (18.3 MΩ). This solution was kept in a closed bottle to prevent the water evaporation during growth. Growth time is used to determine the length of the nanowires. The bottle was dipped into an oil bath kept at 90°C for several hours. This process leads to hydroxide ion formation as a result of the decomposition of HMTA, which reacts with the Zn^{2+} ions to form ZnO crystals. During the nanowire growth process, the following reactions occur:

$$(CH_2)_6N_4 + 6H_2O \leftrightarrow 6HCHO + 4NH_3$$

$$NH_3 + H_2O \leftrightarrow NH_4^+ + OH^-$$

$$Zn + 2\ NH_4^+ \leftrightarrow Zn^{2+} + 2\ NH_3 + H_2$$

$$Zn^{2+} + 2\ OH^- \leftrightarrow Zn(OH)_2 \leftrightarrow ZnO\ (s) + H_2O$$

Firstly, the reaction of HMTA and water occurs and gives ammonia into the solution. Then, ammonia reacts with water and this reaction results in the formation of ammonium and hydroxide ions. Finally, these ions react with Zn ion to form ZnO as indicated before. A photograph of the growth setup used in this thesis is shown in Figure 2.5.

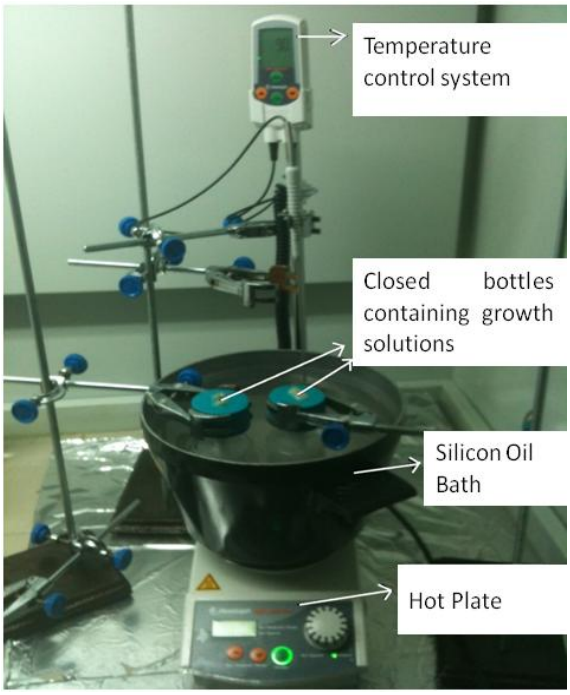

Figure 2.5 Photograph of the hydrothermal growth setup used in the experiments.

Following growth, substrates were removed from the solution, rinsed with DI water to avoid residual salts and dried under nitrogen flow.

2.3 ZnO Nanowire Characterization Methods

2.3.1 Scanning Electron Microscopy (SEM)

The morphology and size of the ZnO nanowires were investigated by FESEM (Nova NanoSEM 430) operated at a voltage of 10 kV. Cross-sectional SEM images were obtained from the cleaved edges of the substrates. No gold or carbon coating was utilized.

2.3.2 X-Ray Diffraction Measurements

The crystal structure of the ZnO nanowires was investigated using X-Ray diffraction (XRD) analysis. A Rigaku D/Max-2000 PC diffractometer was employed, using Cu-Kα radiation (λ=1.54056 Å) at an X-Ray source operating voltage of 40 kV in the 2θ range of 30-60° at a scanning rate of 2°/min.

2.3.3 UV-Visible Spectroscopy

Optical UV-Visible (UV-VIS) absorption measurements were taken using VARIAN CARY 100 BIO UV-Visible Spectrometer in normal incidence mode from ZnO nanowires grown on glass substrates within the wavelength range of 300-800 nm. Bare glass substrates were used as reference.

2.3.4 Photoluminescence Measurements

To investigate the optical characteristics of ZnO nanowires, photoluminescence (PL) measurements were performed using a HORIBA Jobin Yvon PL system at an excitation wavelength of 325 nm. Measurements were conducted at room temperature.

2.4 Results and Discussion

Figure 2.6 (a) and (b), respectively, show top-view and cross-sectional SEM images of ZnO nanowires synthesized through hydrothermal growth. These images revealed that the nanowires were vertically aligned and the length and diameter of the nanowires were 2 μm and 80-100 nm, respectively.

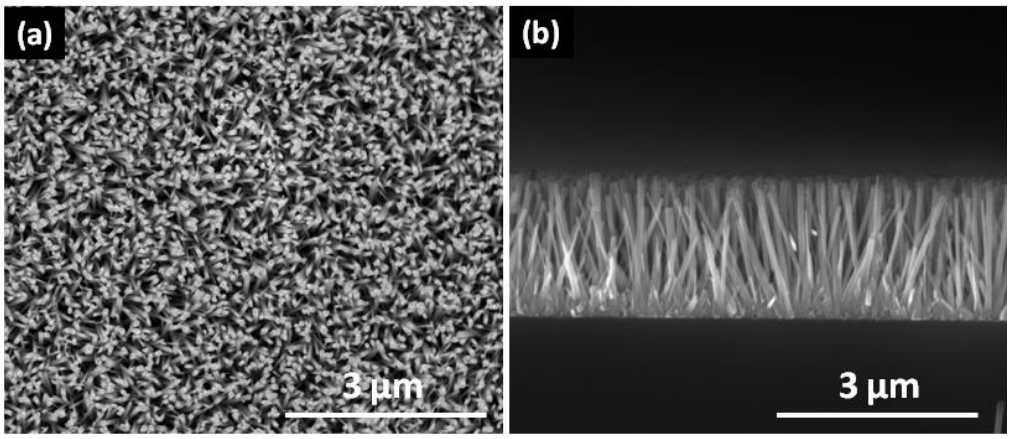

Figure 2.6 (a) Top-view and (b) cross-sectional SEM images of the ZnO nanowires. Magnifications 40000X.

The hexagonal cross-section of the nanowires is an indication of their crystal structure, which was also confirmed by XRD. XRD spectrum of ZnO nanowires grown at 90°C is shown in Figure 2.7. The strong peak at 34.8° (2θ) corresponding to (002) spacing of the wurtzite structure (JCPDS Card No: 36 – 1451) revealed the preferential alignment of the nanowires on the substrate in their c-axis direction.

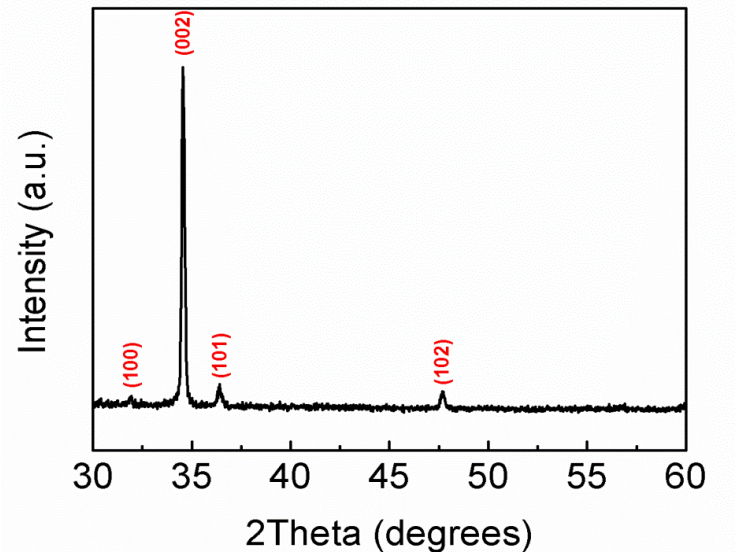

Figure 2.7 XRD spectrum of highly oriented and hydrothermally grown ZnO nanowires.

Figure 2.8 shows the PL spectrum of the nanowires. In order to avoid noise and make emission peaks clear, Gaussian fitting was applied to the PL curve. ZnO generally has two PL peaks, a sharp peak at around 378 nm from the direct band gap transition and a broad peak occurring between 530-580 nm related with the transitions from the defect states.

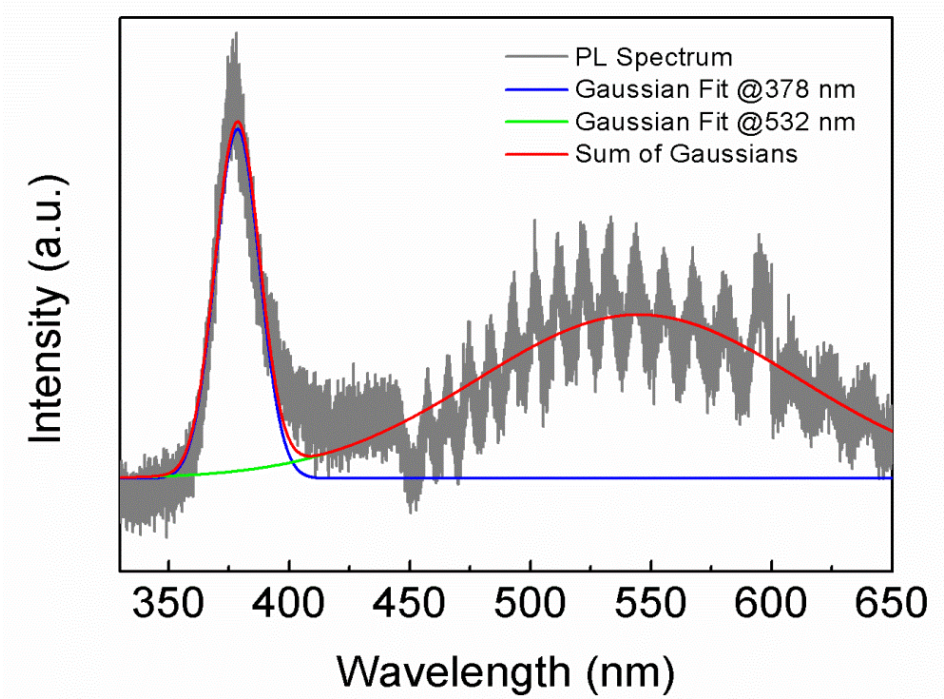

Figure 2.8 PL spectrum of ZnO nanowires with Gaussian fitting.

Figure 2.9 shows the normal incidence transmittance of the hydrothermally grown ZnO nanowires in the 1.5-5 eV photon energy range. In this range, almost constant and high transparency in the visible range and a sharp absorption onset at 378 nm is observed. The bandgap of the ZnO nanowires are estimated to be 3.29 eV from the Tauc plot considering the direct bandgap, as shown in the inset of Figure 2.9.

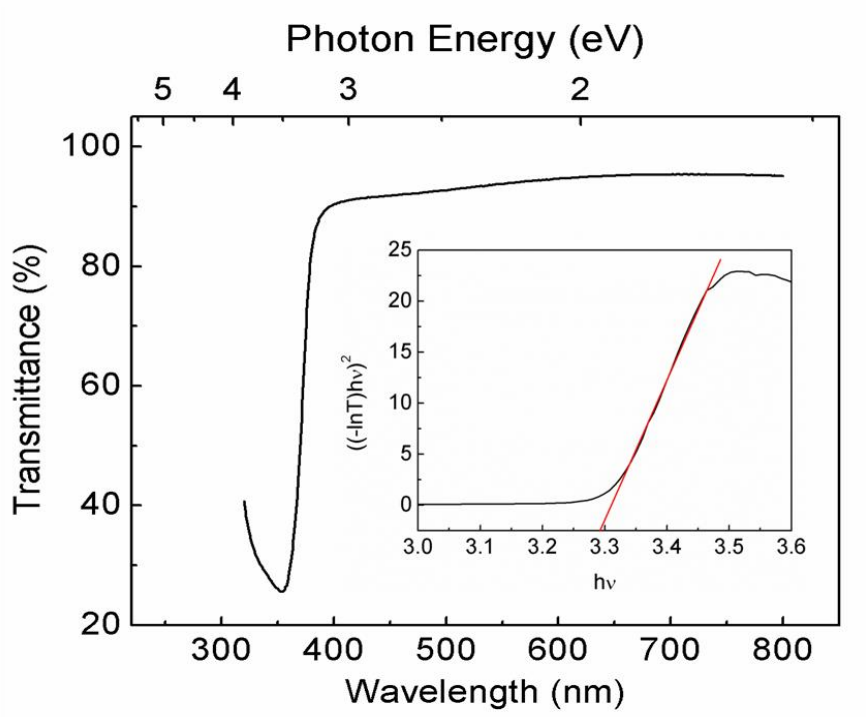

Figure 2.9 Optical transmission spectrum of ZnO nanowires. Inset shows a typical plot of $(\alpha h\nu)^2$ vs energy curve for the samples.

CHAPTER 3

DOPING OF ZnO NANOWIRES BY HYDROTHERMAL METHOD

3.1 Introduction

Semiconducting nanowires are highly appealing materials for optoelectronic devices. A few of the challenges for the industrial scale utilization of semiconducting nanowires in optoelectronic devices are their manipulation, processing, positioning of large amount of nanowires, morphology and doping level control. Additionally, reliable and cost effective techniques for the synthesis large numbers of nanowires should be developed to acquire any benefit from these nanomaterials.

In contrast to the very negative image in sports, doping in semiconductors becomes a key technology for electronic devices. Doping basically includes the process of locally controlling the charge carrier density and conductivity of the semiconductors with the addition of a small percentage of foreign atoms into the regular crystal structure.

Among semiconductors, ZnO has received extra attention due to its high exciton binding energy and ease of nanostructure fabrication. In order to utilize ZnO in various applications, both high quality n- and p-type doping is necessary.

It is known that, ZnO normally reveals n-type behavior in its intrinsic state. By controlling the doping level and also defects if possible, electrical properties of ZnO can be tuned from metallic to insulating state, as well as converting the behavior from n-type to p-type [8]. As in the case of most oxide materials, n-type doping of

ZnO is easy; but it is difficult to be doped p-type [41]. It is highly attractive to make reproducible and stable p-type ZnO for the fabrication of ZnO homojunction optoelectronic devices. p-type doping of ZnO for these reasons are quite challenging and the topic is still under debate.

3.1.2 Doping of ZnO Nanowires

One of the important features of ZnO nanowires is the ability to introduce foreign atoms into the lattice to tune the electrical properties. The ability to control the electronic properties of these nanowires through doping is significant in developing optoelectronic devices.

ZnO nanowires are intrinsically n-type due to the point defects, such as zinc (Zn) intersitials and oxygen (O) vacancies [42]. It is possible to introduce different substitutes and decrease the number of these defects by doping elements with similar electronegativities. Therefore, doping becomes a method of controlling ZnO nanowire properties such as the bandgap and electrical conductivity. In addition, wurtzite ZnO has sp^3 covalent bonding, but it has also a substantial ionic character [8]. As a result, compared to the other covalently bonded wide bandgap semiconductors, such as gallium nitride (GaN), doping in ZnO is much easier.

One of the main issues for the application of ZnO in devices is ambipolar doping. This problem is commonly observed in wide bandgap materials and occurs when doping of one type (for ZnO, n-type conductivity due to electrons in the conduction band) can be easily accomplished, whereas the opposite type (in this case, due to holes in the valence band) is hardly achievable. For instance, ZnO, zinc selenide (ZnSe), cadmium sulfide (CdS), or GaN are generally n-type, whereas zinc telluride (ZnTe) is generally p-type [43].

Different metals and non-metals have been used to dope ZnO nanowires. Some of the examples of metal dopants include nickel (Ni), copper (Cu), silver (Ag), aluminum (Al), gallium (Ga), indium (In) [44-49] and non-metal dopants such as carbon (C), nitrogen (N), phosphorus (P), chlorine (Cl) [50-53]. In addition, co-

doped nanowires with two different elements such as manganese (Mn) + cobalt (Co) [54], Mn + lithium (Li) [55], Li+N [56] have also been investigated by some research groups.

The foreign atoms can be introduced into the ZnO lattice similar to n and p-type doping of silicon. One approach can be the substitution of Zn with Group III elements (Al, Ga, In) or the replacement of O with Group VII elements (F, Cl) for n-type doping [7]. Another mechanism includes the substitution of Zn with Group I or IB elements (Li, Na, K, Cu, Ag) or the substitution of O with Group V elements (N, P, As) for p-type doping.

Al, Ga and In, which are known as the most common dopants used to achieve n-type doping, act as shallow donors in ZnO structure. Al^{3+}, Ga^{3+} and In^{3+} cations have higher valence state than Zn^{2+}, which provides an electron carrier.

To achieve p-type doping, the dopant, having a lower valence than Zn, should introduce a shallow acceptor level in the bandgap of ZnO. It was revealed that Group I elements could be preferable p-type dopants compared to Group V elements in terms of shallowness of acceptor levels [57]. However, Li and Na, as Group I elements, tend to occupy interstitial sites instead of substitutional ones due to their small atomic radii and therefore they act as donors rather than acceptors [8]. Although p-type doping in ZnO thin films is still controversial, p-doping in ZnO nanowires appears promising due to the absence of dislocations [37].

Generally, acceptors or donors should have an ionic radius close to the host ion so as to maintain continuity of the crystal lattice. Moreover, doping elements should have similar electronegativities to energetically favor their incorporation to the lattice. Table 3.1 gives the atomic radii and valence of different kinds of dopant elements for ZnO.

Table 3.1 Valence and ionic radii for candidate donors and acceptors for ZnO [43].

Atom	Valence	Ionic Radius (Å)
Zn	2+	0.60
Al	3+	0.39
Ga	3+	0.47
In	3+	0.62
Li	1+	0.59
Na	1+	1.13
K	1+	1.51
Cu	2+	0.71
Ag	1+	1.00
P	3+,5+	0.58,0.34
As	3+,5+	0.58,0.47
Mn	2+	0.80
Co	2+	0.38
Ni	2+	0.55
Fe	2+,3+	0.77,0.63
O	2-	1.38
N	3-	1.46
P	3-	2.12
As	3-	2.22
F	1-	1.31

There are some difficulties in p-type doping of ZnO due to different mechanisms such as low solubility of p-type dopants, compensation of dopants with native defects and formation of deep acceptor levels [57]. As a matter of fact, successful p-type doping for ZnO nanostructures will greatly improve their future applications in nanoscale optoelectronics.

Besides controlling the conductivity type of ZnO, different physical properties can be imparted through transition metal doping. For instance, ZnO nanowires can show ferromagnetic behavior when doped with transitions metals. Transition metal doped dilute magnetic semiconductors (DMSs) are one of the most popular research fields

for potential applications, especially in spintronic devices and visible light photocatalysis [37].

3.1.3 Applications of Doped ZnO Nanowires

Doping is the basic technique to control physical properties of ZnO nanowires such as bandgap, type of majority carriers, electrical conductivity and ferromagnetism [7]. To date, different kinds of dopants have been introduced into the ZnO lattice to utilize them in various applications.

In recent years, transition metal doped ZnO nanowires attract great attention for their novel magnetic properties. These structures are generally called DMSs and as mentioned before, they are promising and potential building blocks for spintronic devices. Generally, the ferromagnetic behavior of ZnO depends on the dilute doping of 3d transition metal ions (e.g. Mn, Co, Cu) into the structure. It is claimed that, the partially filled d states consist of unpaired electrons and are responsible from this behavior due to their spin. Basically, when these 3d transition metal ions are replaced with the cations of the host, the electronic structure is influenced by strong hybridization of 3d orbitals of the metal ion and by the p orbitals of the neighboring host anions. Strong magnetic interaction between localized 3d spins and the carriers in the host valence band occurs due to this hybridization [58]. However, in spite of various studies including this issue, the origin of the ferromagnetism is still under debate. In addition, the magnetic metals such as Mn and Co in ZnO structure can be proposed as the source of the ferromagnetism. In order to sort out this problem of magnetic precipitates in a DMS, Cu doping has become an excellent approach, because both Cu and its oxide compounds are nonmagnetic [59].

In a related research, Xu et. al. reported a comparative study of the ferromagnetism in undoped and Cu doped ZnO (ZnO:Cu) nanowires grown by a vapor transport route. Figure 3.1 shows the magnetization (M-H) of undoped and ZnO:Cu nanowires at 293 K [60].

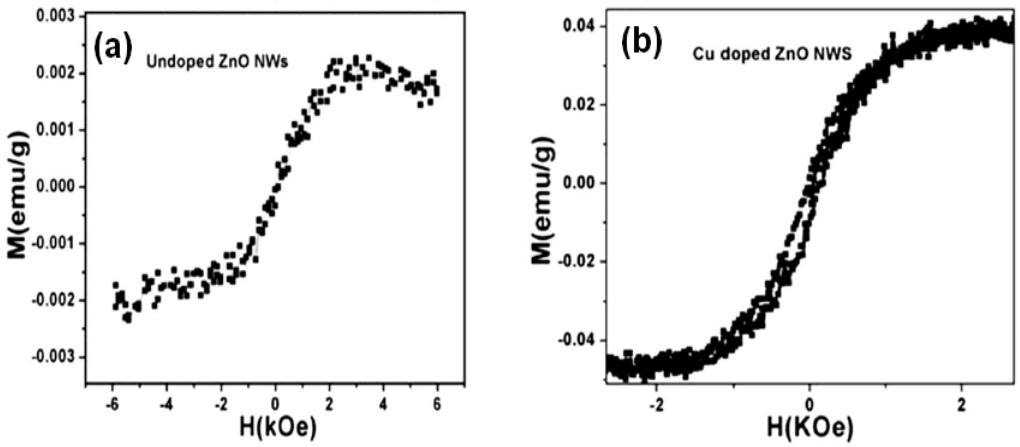

Figure 3.1 M-H curves of (a) undoped and (b) ZnO:Cu nanowires measured at room temperature [60].

The magnetic properties of the samples were investigated by superconducting quantum interference device. The magnetization of undoped ZnO nanowires was calculated to be 20 times smaller but not zero as compared to the doped counterpart. This result was attributed to the Zn clusters embedded in the ZnO matrix. On the other hand, for ZnO:Cu nanowires, an evident ferromagnetic hysteresis loop with a magnetization of 4.1×10^{-2} emu/g was obtained due to the effect of defects involving Cu dopants and Zn intersitials [60].

To obtain p-type ZnO, various dopant sources have been investigated. A related research revealed that Ag substitution in ZnO decreases the donor density, which revealed that Ag can be an effective acceptor [61]. In addition, nanowires can be shown as appropriate candidates to explore p-type doping of ZnO with their single crystal structures. Song et. al. provided a study on ZnO:Ag nanowires using VLS mechanism. The concentration of Ag was adjusted to be between 1–5 wt%. Low temperature PL spectrum was examined to verify the doping status. In addition, a homojunction, all-ZnO diode was demonstrated including 3 wt% ZnO:Ag nanowire clusters and n-type ZnO:Ga thin film. Figure 3.2 (a) and (b) show the low temperature PL data of 3 wt% ZnO:Ag nanowires and the I-V characteristics of the diode, respectively [62].

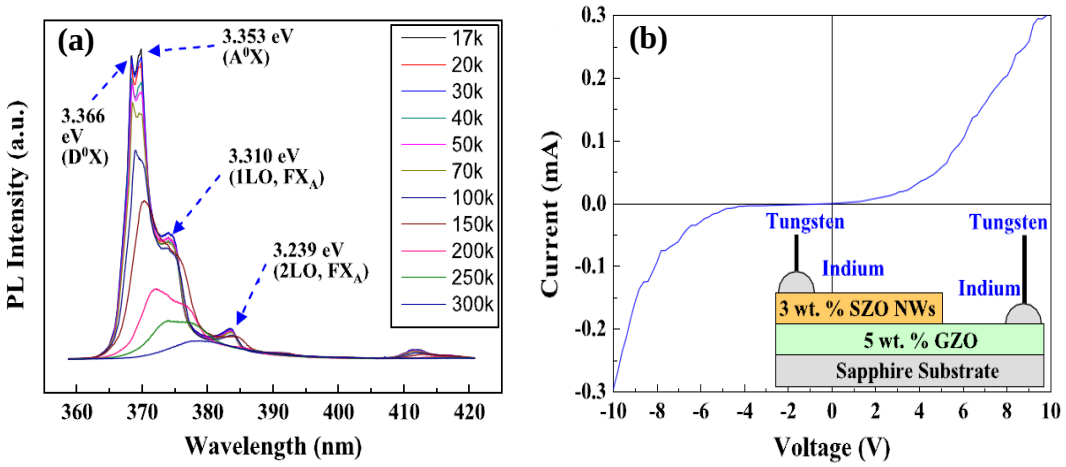

Figure 3.2 (a) Low temperature photoluminescence data for the 3 wt% ZnO:Ag nanowire cluster and (b) I–V characteristics of a diode with ZnO:Ag nanowires and ZnO:Ga thin film [62].

PL analysis has been conducted at 17K to reveal the exciton peaks. The peaks at 3.37 eV and 3.35 eV were referred to the donor-bound excitons and the acceptor-bound excitons, respectively. On the basis of these results, the acceptor-bound exciton peak confirmed p-type behavior of ZnO. In addition, I-V characteristics of the diode yielded an asymmetric curve. The ideality factor calculated from the diode was much higher than conventional thin film diodes, which normally have n values ranging from 1 to 7. In addition, no sharp edge was observed in the I-V curve. These results were attributed to the leakage paths at the p-n interface. The leakage paths could originate from the surface imperfections and cause short circuit [62].

Conductivity enhancement of ZnO by doping is also an attractive application area. ZnO:Al, as an alternative transparent conductive oxide to indium tin oxide (ITO), has gained great interest due to its unique optoelectronic properties as well as non-toxicity and low cost. Although much work has been performed on ZnO:Al thin films, there are only few studies on the synthesis and characterization of ZnO:Al nanowires. Lin et. al. provided a study on a photoconductor device consisting of a single ZnO:Al nanowire. The nanowires were synthesized by electrospinning

process. Figure 3.3 shows the device schematic and I-V characteristics of undoped and ZnO:Al samples [63].

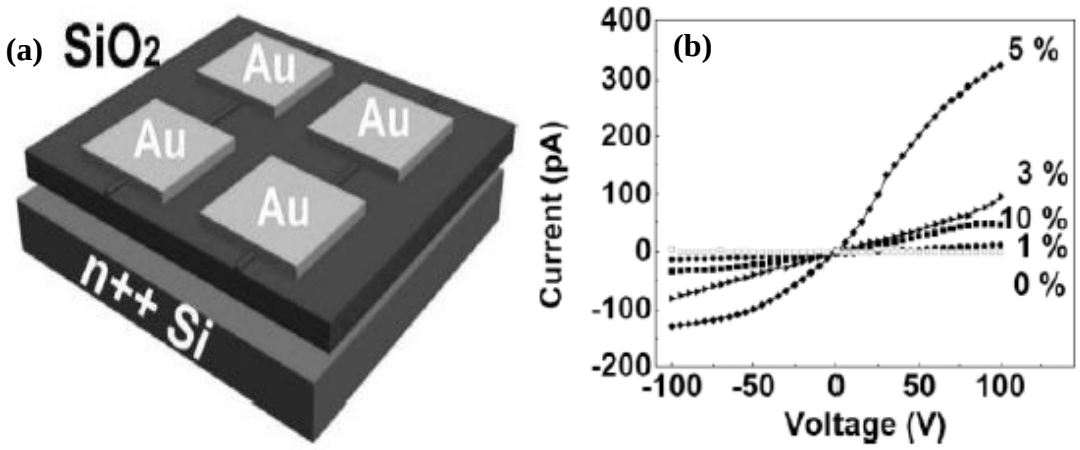

Figure 3.3 (a) Schematic illustration of device configuration for electrical measurements and (b) I–V characteristics of undoped and ZnO:Al samples [63].

I-V measurements of undoped and ZnO:Al nanowires with different Al concentrations were carried out and conductivity calculations were made. The conductivity of undoped nanowire was 2.55×10^{-5} $S.cm^{-1}$, while Al doped ones showed an increase up to 9.73×10^{-3} $S.cm^{-1}$, indicating an enhancement in the conductivity. Basically, Al is a cationic dopant for ZnO lattice and the trivalent Al^{3+} ion occupies the sites for divalent Zn^{2+}, so that electrons can easily move to the conduction band. This results in an increase in the number of electrons and improves the conductivity. In addition, from the photoconductivity measurements of ZnO:Al nanowires, it was observed that the conductivity was 20 times higher when exposed to below-gap light as compared to dark [63].

3.1.4 Doping Methods of ZnO Nanowires

n and p-type doping have been achieved in semiconductor nanowires via different routes including in-situ doping during growth [64], post-annealing [65] and ion implantation [66]. However, some of those approaches have inherent problems. For instance, post-annealing leads to a decrease in near band edge emission intensity owing to dopant contamination of nanowires [65]. Ion implantation leads to high defect density and damage, which results in low quality crystal structure and high resistivity in nanowires [67]. In addition, it becomes difficult to control doping and electrical properties of nanowires by post-annealing and ion implantation processes. Compared to these techniques, in-situ doping approach yields much better results in terms of controlled doping profile with manageable growth parameters while keeping the high quality nanowire structure [41].

To date, various methods such as CVD, thermal evaporation, electrodeposition and hydrothermal growth have been used for the controlled synthesis and in-situ doping of ZnO nanowires. Dopants in these methods are incorporated into ZnO nanowires during wire growth. In vapor phase synthesis methods, the dopant is carried into the reaction furnace along with the constituent precursors, while in solution phase synthesis techniques, it is codissolved with other precursors at the beginning of the reaction. Although semiconductor nanowires are generally synthesized and doped using vapor phase methods, in-situ doping via solution based methods has unique advantages including low cost, mass production possibility and simplicity. Furthermore, solution phase reactions generally occur at relatively low temperatures compared to vapor phase synthesis methods.

In hydrothermal method, small amounts of dopant metal salts are added to the growth solution. These additives do not hinder ZnO nanowire growth, unless the pH value of the growth solution is seriously altered. It is expected that, the existence of other ions leads to the incorporation of dopants into the ZnO structure.

In the following part, synthesis and characterization of doped ZnO nanowires using hydrothermal growth method is reported. The metal dopants such as Cu, Ag and Al were used to dope ZnO nanowires.

3.2 Experimental Details

Silicon (Si) wafer, soda-lime silica glass and indium tin oxide (ITO) coated glass slides (Delta technologies, Rs: 4-8 Ω) were used as the substrates for the growth of doped ZnO nanowires. Substrates were first cleaned to remove organic residues according to the procedure mentioned before in the Chapter 2. All chemicals were purchased from Sigma-Aldrich and used without further purification.

ZnO nanowires were doped with three different elements, namely copper (Cu), silver (Ag) and aluminum (Al). Doping procedure included the addition of Cu (II) acetate monohydrate, Ag acetate or Al acetate with different concentrations into the growth solutions. Following ZnO seed layer deposition, the substrates were immersed into equimolar (20 mM) aqueous solution of metal acetates (zinc and dopant) and HMTA in DI water (18.3 MΩ) and nanowires were grown using the method described in the previous chapter.

The p-n homojunctions were produced as follows; initially, ITO coated glass substrates with ZnO seed layer were dipped into standard or Al acetate added growth solution and heated there for 1.5 hours. After that, the samples were immediately immersed into a new growth solution prepared with Ag acetate addition for another 1.5 hours.

For electrical measurements, doped ZnO nanowires were grown on ITO coated glass substrates and an insulating polymer solution was infiltrated between the nanowires in order to prevent short circuits between the top metal contact and ITO. Polystyrene (PS, Mw ~ 280,000, Sigma Aldrich) was used as the insulating polymer. PS solution was spin coated onto the nanowires. This procedure can be carried out a number of times depending on the required thickness. After each coating, annealing at 120 °C and ultraviolet curing were done to coated polymer layers. Following polymer coating, the oxygen plasma etching was carried out to release the nanowire tips, so then the proper top contact can be deposited.

After the oxygen plasma treatment, Al or nickel/Gold (Ni/Au) top contacts were deposited by a thermal evaporator using appropriate shadow masks. During

evaporation, the chamber was vacuumed down to a base pressure of $1x10^{-6}$ mbar. A large current was passed through a tungsten boat in order to melt the metal pellets. Then the metal was evaporated and condensed on top of the substrate with a pattern dictated by the shadow mask.

3.3 Doping Characterization Methods

3.3.1 Scanning Electron Microscopy (SEM)

Morphology of the doped ZnO nanowires were analyzed by FESEM (Nova NanoSEM 430) operated at a voltage of 10 kV. Cross-sectional SEM images were obtained from cleaved edges of the substrates. Polymer containing substrates were coated with gold to prevent charging.

3.3.2 X-Ray Diffraction Measurements

The crystal structure of the doped ZnO nanowires was investigated using X-Ray diffraction (XRD) analysis. A Rigaku D/Max-2000 PC diffractometer was employed, using Cu-Kα radiation (λ=1.54056 Å) and X-Ray source operating voltage of 40 kV in the 2θ range of 30-80° at a scanning rate of 0.02°/min.

3.3.3 UV-Visible Spectroscopy

Optical UV-Visible (UV-VIS) absorption measurements were taken using VARIAN CARY 100 BIO UV-Visible Spectrometer in normal incidence mode from undoped and doped ZnO nanowires grown on glass and ITO coated glass substrates within a wavelength range of 300-800 nm. Bare glass or ITO coated glass substrates have been used as the reference.

3.3.4 X-Ray Photoelectron Spectroscopy (XPS)

Kα monochromated high-performance XPS spectrometer was used for the analysis of the undoped and doped ZnO nanowires. XPS analysis has been performed for the examination of the existence of the dopant elements. Nanowires grown on Si substrates were directly subjected to analysis without any special sample preparation procedure. All of the XPS spectra shown here have been calibrated with respect to carbon signal.

3.3.5 Vibrating Sample Magnetometer (VSM)

The magnetic properties of Cu doped ZnO nanowires were characterized by ADE Magnetics EV/9 model Vibrating Sample Magnetometer (VSM). VSM operating system is based on the detection of a dipole field from a magnetic sample when it is vibrated perpendicularly to a uniform magnetic field.

3.3.5 Photoluminescence Measurements

To investigate the optical characteristics of undoped and doped ZnO nanowires, photoluminescence (PL) measurements were performed using a HORIBA Jobin Yvon PL system at an excitation wavelength of 325 nm. Measurements were conducted at room temperature. Gaussian fitting was applied to PL curves.

3.3.6 Current-Voltage Measurements

I-V measurements were carried out using a Keithley 2400 sourcemeter as the voltage source. Voltage was swept between negative to positive values and corresponding current values were recorded using a Labview program.

3.4 Results and Discussion

Cu, Ag and Al were selected as metal dopants due to their effect on the magnetic properties, p-type conduction and electrical conductivity of ZnO nanowires, respectively.

3.4.1 Copper Doping of ZnO Nanowires

Figure 3.4 (a) shows a top-view SEM image of Cu doped ZnO (ZnO:Cu) nanowires grown in a solution containing 5 mM Cu acetate+15 mM Zn acetate + 20 mM HMTA. Typical wurtzite hexagonal structure of ZnO nanowires with an average diameter of 150 nm can be seen clearly from the image. Figure 3.4 (b) shows energy dispersive X-Ray spectroscopy (EDX) results for the same sample. In addition, the EDX result indicates the presence of Zn, O, and Cu in the structure. This result can be attributed to the incorporation of Cu into the ZnO nanowires.

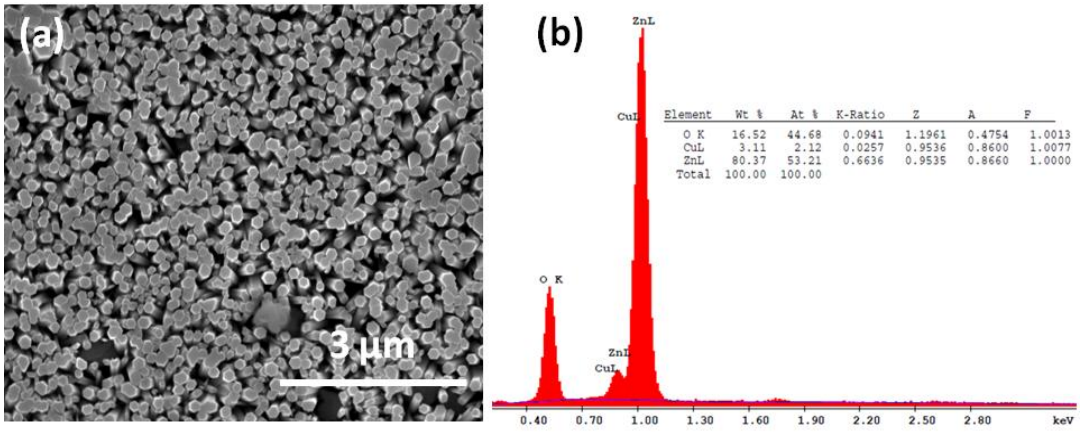

Figure 3.4 (a) Top-view SEM image and (b) corresponding EDX spectrum of ZnO:Cu nanowires.

Figure 3.5 shows the XRD pattern of ZnO:Cu nanowires. XRD pattern of undoped nanowires have been also provided for comparison. Both patterns can be indexed with the hexagonal wurtzite structure without any detectable impurities (JCPDS Card No: 36 – 1451). This indicates that the wurtzite structure of the ZnO nanowires has been preserved through Cu doping and Cu was incorporated into the ZnO lattice without any phase segregation.

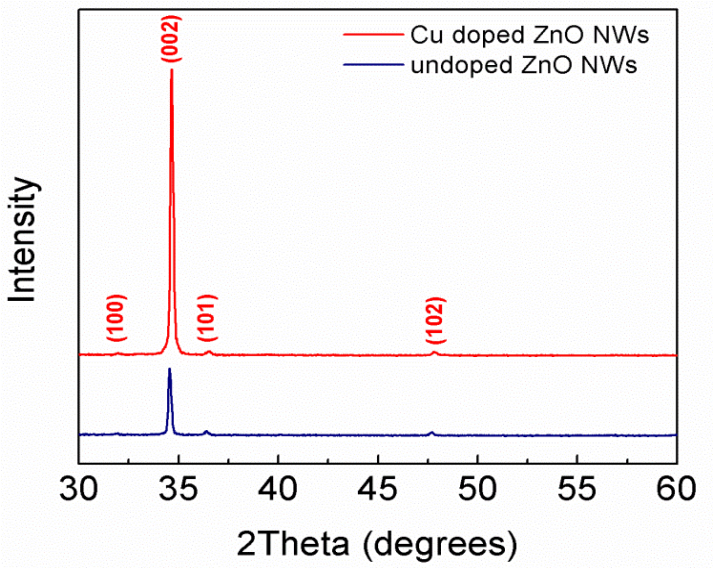

Figure 3.5 XRD patterns of undoped and Cu doped ZnO nanowires.

XPS results of undoped and ZnO:Cu nanowires are shown in Figure 3.6. XPS was used to determine the doping concentration and the valence state of Cu in the doped nanowires. The emission peaks at 1022.1 and 1045.1 eV are from the Zn ($2p_{1/2}$) and ($2p_{3/2}$) core levels, respectively, and the peak at 531 eV is from O (1s). From the inset of Figure 3.6, the peaks related to Cu ($2p_{3/2}$) and Cu ($2p_{1/2}$) are located at about 932.5 and 952.3 eV, respectively, which indicates that the valence state of Cu in the nanowires is +2 and a bond between Cu 2+ and O 2− is formed. The electron emissions from Zn (3s), (3p), and (3d) core levels are also observed.

In addition, the results were calibrated by taking the binding energy of the C (1s) peak (285.0 eV) as the reference in XPS. The appearance of C (1s) peak in the XPS spectrum is observed due to the hydrocarbon contamination on the sample surface following air exposure. The carbon signal can be considerably reduced through Ar ion etching.

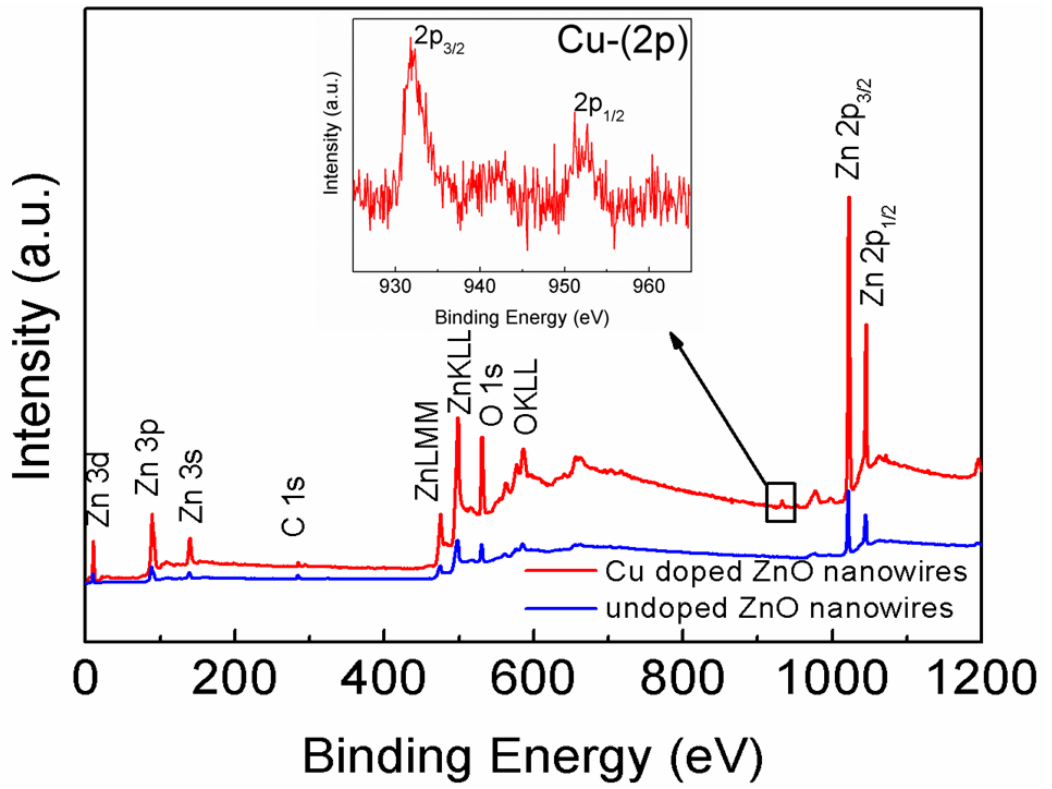

Figure 3.6 XPS survey scan and high-resolution scan (inset) of Cu ($2p_{3/2}$) and ($2p_{1/2}$) peaks measured on ZnO:Cu nanowires.

Figure 3.7 shows magnetization versus magnetic field (M–H) curves measured on undoped and ZnO:Cu nanowires grown on Si wafer. To investigate the effect of annealing on magnetic properties of ZnO:Cu nanowires, samples were annealed at 350°C for 1 hour.

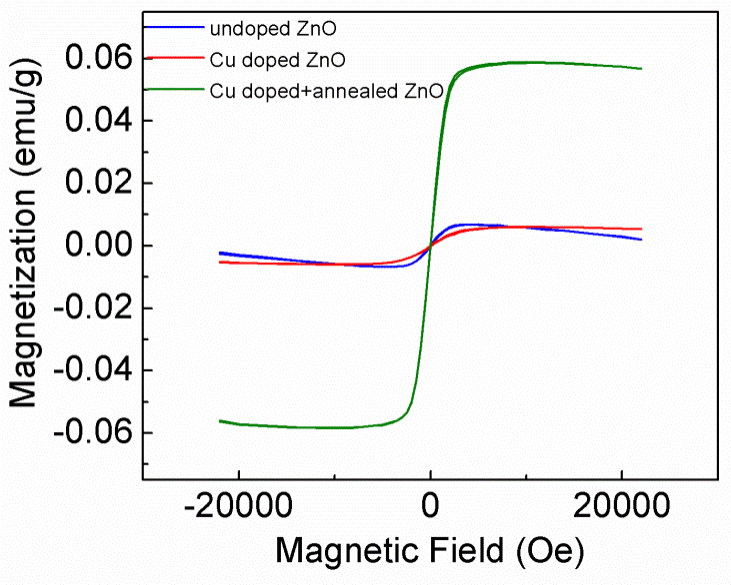

Figure 3.7 M-H curves of undoped and ZnO:Cu nanowires measured at room temperature.

From the M-H curves, it can be seen that the saturation magnetization values of undoped, Cu doped, Cu doped and annealed ZnO nanowires are 0.002 emu/g, 0.005 emu/g and 0.056 emu/g, respectively. These results indicate that, the ferromagnetic behavior of ZnO:Cu nanowires is enhanced by annealing. This enhancement can be attributed to the influence of Zn intersitials and O vacancies due to annealing resulting in the homogeneous distribution and the activation of Cu atoms in the structure.

3.4.2 Silver Doping of ZnO Nanowires

SEM image of the ZnO:Ag nanowires is shown in Figure 3.8 (a). As it can be seen, similar to undoped ones, ZnO:Ag nanowires have hexagonal structure Results of the EDX analysis is provided in Figure 3.8 (b). The appearance of Zn, O and Ag in the EDX spectrum confirms that Ag ions were introduced into ZnO nanowires. A strong Si signal is due to the substrate.

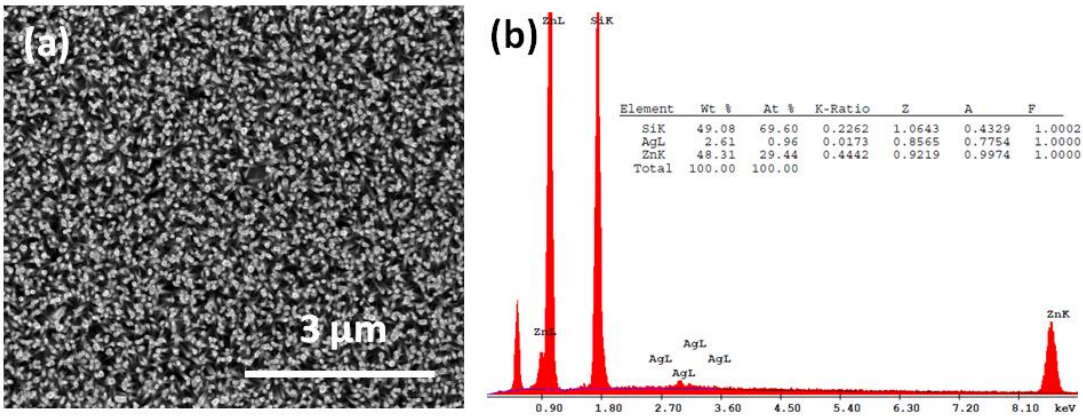

Figure 3.8 (a) SEM image and (b) EDX results of ZnO:Ag nanowires grown on Si substrate.

XRD spectrum for the ZnO:Ag nanowires is shown in Figure 3.9. Spectrum for the undoped nanowires was also provided for comparison. All diffraction peaks can be indexed with the hexagonal wurtzite structure of ZnO (JCPDS Card No. 036-1451).

From the XRD spectra of both undoped and ZnO:Ag samples, it can be seen that the wurtzite structure of ZnO nanowires has not been changed with the addition of Ag. Moreover, some additional peaks at 33, 38.1 and 44.3 degrees attributed to metallic Ag or Ag_2O (200) are observed in doped samples. This can be due to residual Ag particles within the nanowires. In Figure 3.9 inset, the comparison of (002) and (101) peaks is shown. There is a 0.12° shift towards lower 2θ values within the XRD diffraction peaks for ZnO:Ag nanowires as compared to undoped ones. Since the radius of Ag^{1+} ion is greater than Zn^{2+}, lattice expansion occurs in ZnO:Ag samples. To examine the peak shifts, XRD spectra of both undoped and ZnO:Ag samples were calibrated according to the Si peak at 69.36°.

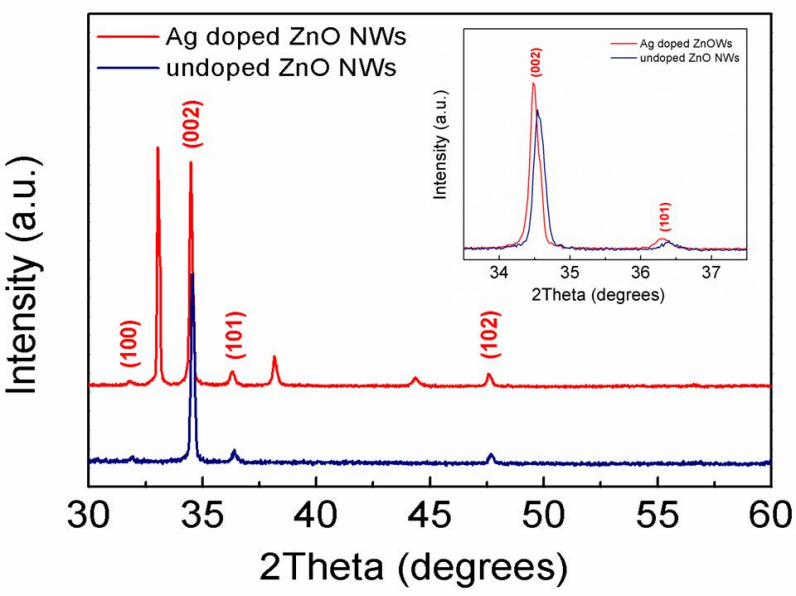

Figure 3.9 XRD patterns of pure and ZnO:Ag nanowires. Inset includes high resolution (002) and (101) peaks of pure and Ag doped samples.

High resolution XPS spectrum for ZnO:Ag nanowires is shown in Figure 3.10. The Ag (3d) binding energy region consists of two signals at 366.4 and 372.3 eV. The signal at 366.4 eV corresponds to Ag ($3d_{5/2}$), and the one at 372.3 eV corresponds to Ag ($3d_{3/2}$). This result can be attributed to the existence of Ag_2O [68].

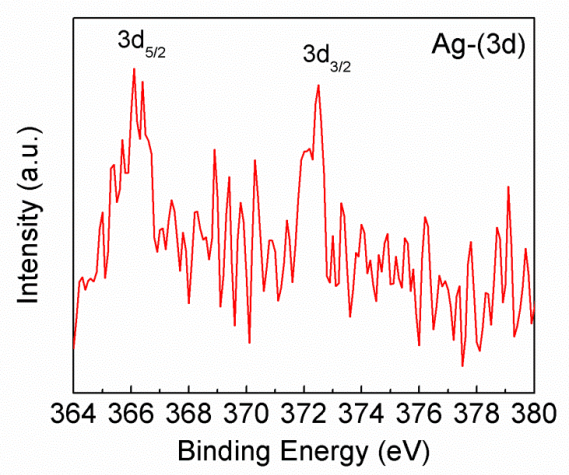

Figure 3.10 High resolution regional XPS spectrum of Ag (3d).

The transmittance spectrum of ZnO:Ag nanowires grown on ITO coated glass substrates is provided in Figure 3.11 (a). Spectrum for undoped nanowires is also provided within the same figure for comparison. In the UV region, the optical transmittance of both undoped and ZnO:Ag nanowires decreases due to the initiation of the fundamental absorption in this region. The change in the transmission of doped samples can be attributed to the effect of doping elements in the structure. Tauc plots obtained from transmittance spectra are shown in Figure 3.11 (b). The optical bandgaps of the samples were found through extrapolating the $((-\ln T)h\nu)^2$ for a direct bandgap semiconductor towards the photon energy axis. A change in the optical bandgap of ZnO:Ag nanowires is observed. The calculated bandgaps of undoped and ZnO:Ag nanowires are 3.33 eV and 3.26 eV, respectively. The reduction in bandgap of doped samples can be related with the formation of acceptor levels within the gap [69].

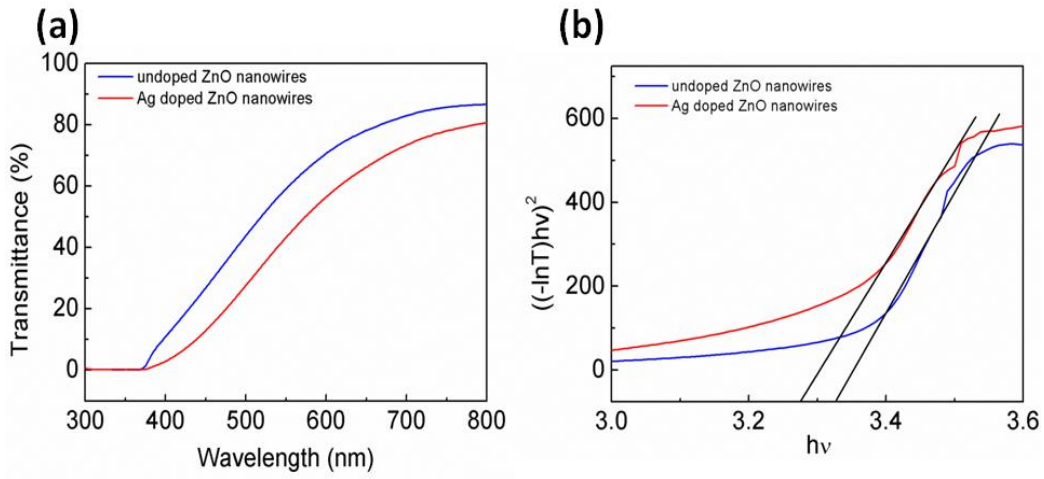

Figure 3.11 (a) UV-VIS spectra of undoped and ZnO:Ag nanowires grown on ITO coated glass substrate and (b) corresponding Tauc plot for undoped and ZnO:Ag samples.

Figure 3.12 shows room temperature PL spectra of both undoped and ZnO:Ag samples. The peaks at approximately 378 nm wavelength are related to UV band

edge emission of ZnO. No considerable change in the position of this UV band has been observed from Ag doped samples. It can be seen that the intensity of these peaks for ZnO:Ag nanowires is much stronger than the undoped nanowires. This indicates that Ag doping enhances the efficiency of exciton recombination [70].

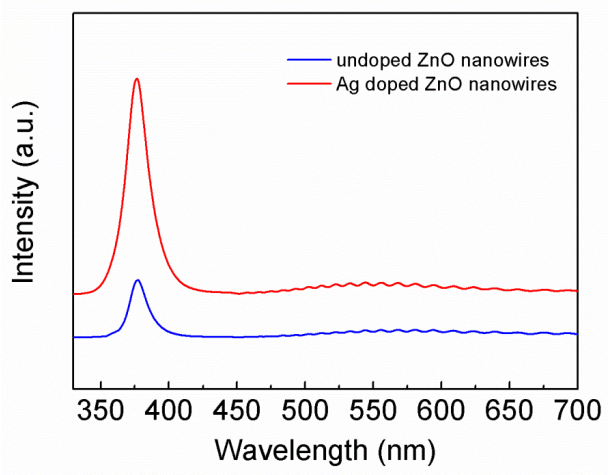

Figure 3.12 PL spectra of undoped and ZnO:Ag nanowires.

To investigate p-type conduction of ZnO:Ag nanowires, p-n homojunction diodes were fabricated. Diodes included undoped or ZnO:Al nanowires as the n-type part and ZnO:Ag nanowires as the p-type section. For Ag doping, 1 mM or 5 mM Ag acetate was dissolved in growth solution. For Al doping, 1 mM Al acetate was added to the growth solution. ZnO:Al nanowires were used to enhance n-type conductivity. Doping with Al is analyzed later in this chapter.

The homojunctions were prepared by growing the ZnO:Ag nanowires on the n-type ZnO nanowires under the same conditions and insulating polymer was coated between nanowires, as mentioned earlier. Ohmic contacts were fabricated by evaporation of Ni (20 nm) - Au (110 nm) on p-type nanowires.

In Figure 3.13, (a) the schematic representation of homojunctions, SEM image of insulating polymer coated nanowires and the photograph of the diode are shown.

Figure 3.13 (b) gives the I-V characteristics of the p-n homojunction diodes within a voltage range of -2V and +2V.

All types of homojunctions yield symmetric I-V curves, which mean no rectification can be obtained. There could be many reasons for these results. Although there is insulating polymer layer between nanowires, some gaps may remain causing short circuit between top and bottom contacts. Another reason can be related with the activation of the dopants in the structure. Annealing of the doped samples can lead to the activation of Ag atoms. However, the diodes cannot be heated to high temperatures due to the presence of polymer layer and ITO. In addition, p-type conductivity may not be stable and could get converted back to n-type after some time [71].

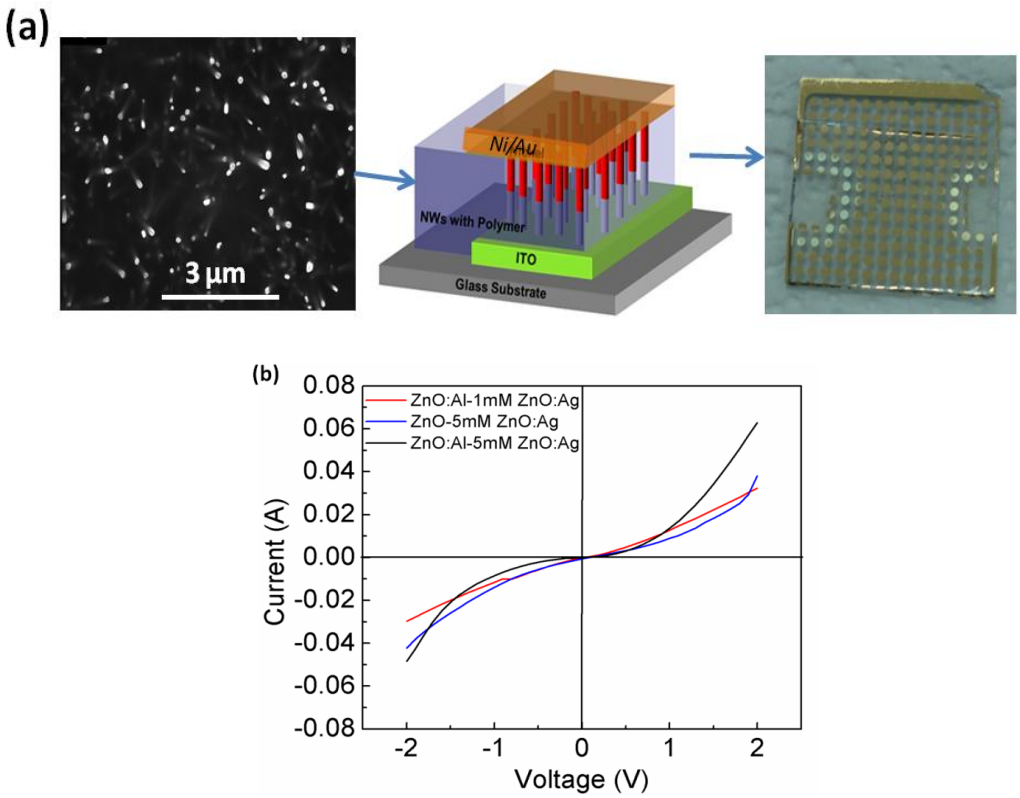

Figure 3.13 (a) Schematic representation of p-n homojunctions with SEM image of polymer coated nanowires and photograph of the diode, (b) I-V characteristics of p-n homojunctions composed of undoped ZnO nanowires/ ZnO:Ag nanowires and ZnO:Al nanowires/ ZnO:Ag nanowires.

3.4.3 Aluminum doping of ZnO Nanowires

Figure 3.14 (a) and (b) show top-view SEM image and the EDX results of ZnO:Al nanowires, respectively. It is seen that ZnO:Al nanowires also have wurtzite structure and no change in hexagonal morphology is observed. From the EDX spectrum, the existence of Zn, O and Al is confirmed.

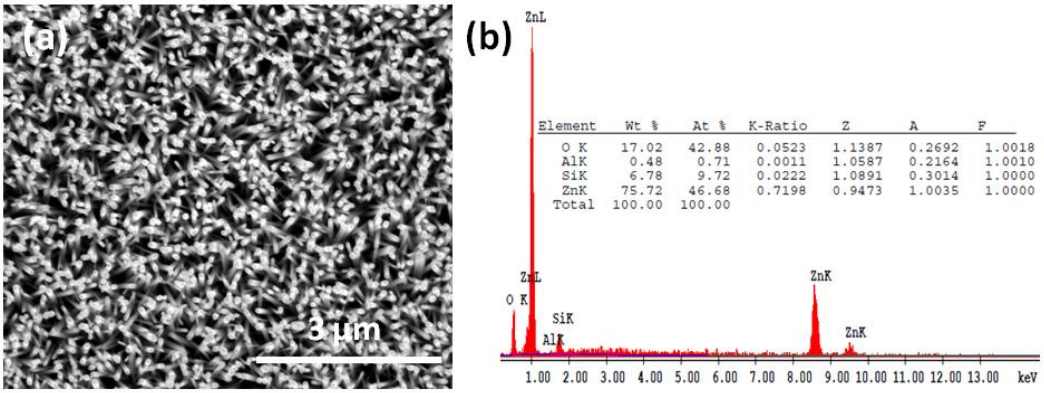

Figure 3.14 (a) SEM image and (b) EDX spectrum of ZnO:Al nanowires grown on Si substrate.

Figure 3.15 depicts the XRD spectra of both undoped and ZnO:Al nanowires. It can be seen that, the preferred orientation of pure and ZnO:Al nanowires was in the (002) direction. The inset of Figure 3.15 shows high resolution XRD spectra of the two samples. Al doping leads to a 0.1° peak shift in 2θ from the wurtzite structure to higher values. This can be due to the substitution Al 3^+ ions for Zn 2^+ ions in the ZnO lattice. The ionic radius of Al 3^+ is 0.39 Å, which is smaller than Zn 2^+ (0.60 Å). The incorporation of Al into the structure leads to a reduction in the lattice parameter of ZnO and results in a peak shift [72].

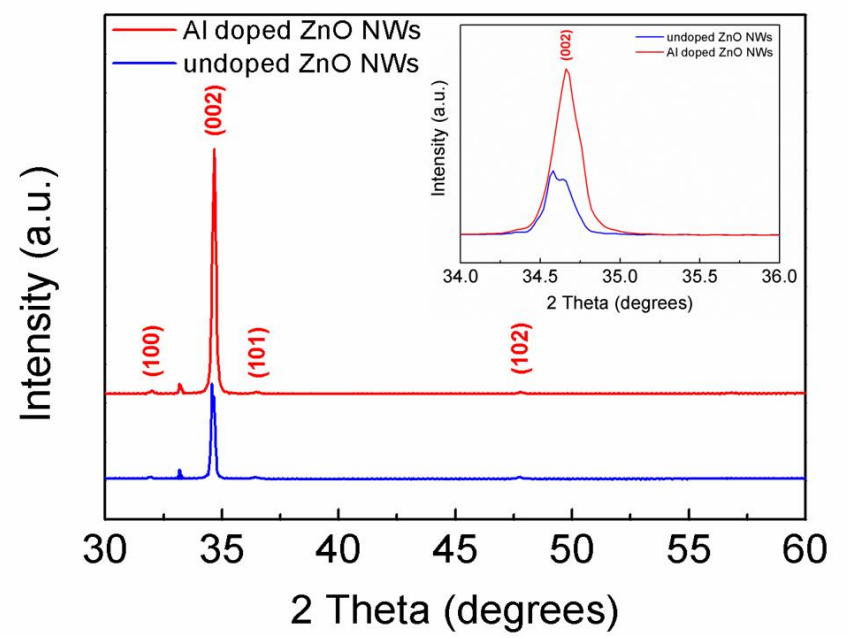

Figure 3.15 XRD patterns of pure and ZnO:Al nanowires. Inset includes the high resolution (002) peak of pure and ZnO:Al samples.

Figure 3.16 shows the room temperature PL spectra of the undoped and ZnO:Al nanowires grown on Si wafer. The strong PL peak observed at 378 nm from undoped ZnO nanowires and the peak observed at 382 nm from ZnO:Al nanowires are both related with the ZnO band edge transition. The broad green emission around 600 nm can be attributed to the transitions from defect states. In addition, UV peak shift due to Al doping show the bandgap reduction. It is known that the Al doping in ZnO have a tendency to reduce the bandgap due to increased carrier concentration. Al donor states located below the conduction band can lead to an impurity band, which overlaps with the bottom of the conduction band, reducing the effective band width [73].

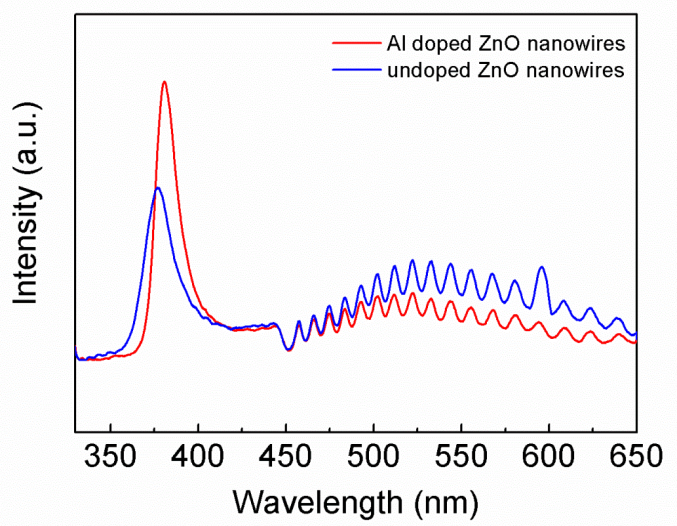

Figure 3.16 PL spectra of undoped and ZnO:Al nanowires.

Figure 3.17 shows the high resolution XPS spectrum including Al (2p) core shell levels. The binding energy of 74.7 eV is attributed to the Al-O bonds. Although the (2p) peak, which is located at 74.7 eV, is not sharp, it indicates that some Al dopant is incorporated into the ZnO lattice.

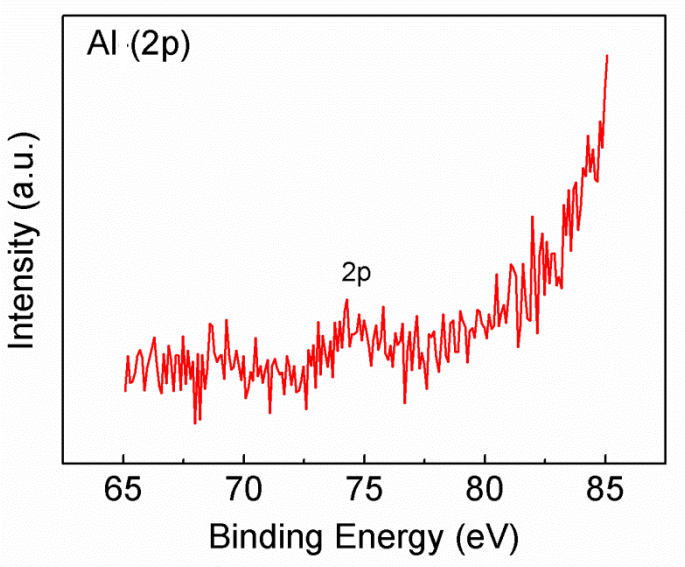

Figure 3.17 High resolution regional XPS spectrum of Al (2p).

Figure 3.18 reveals the I-V characteristics of both pure and ZnO:Al nanowires. To carry out these electrical measurements, Al was evaporated onto the nanowires as the top ohmic contact. Compared to the undoped ZnO nanowires, ZnO:Al ones show higher current values, indicating the enhancement in conductivity. The Al^{3+} ion, which occupies the Zn^{2+} ion site, allows electrons to transfer to the conduction band easily. This means that, Al doping is an effective way to enhance the electrical conductivity of the ZnO nanowires.

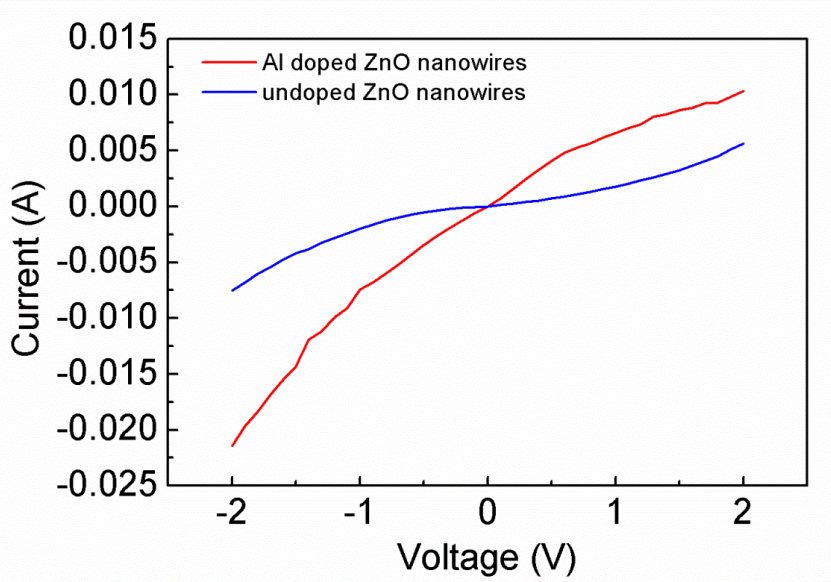

Figure 3.18 I-V characteristics of undoped and ZnO:Al nanowires.

In Table 3.2, the calculated resistance values of pure and Al doped nanowires are given. The results show that, undoped ZnO nanowires have a resistance of 1360 Ω and Al doped ones have 147 Ω. The improved conductivity of the ZnO:Al nanowires can be attributed to the existence of Al in the structure.

Table 3.2 Resistance calculations of undoped and ZnO:Al nanowires.

Al doped ZnO Nanowires			**Undoped ZnO Nanowires**		
V (V)	**I (A)**	**R (Ω)**	**V (V)**	**I (A)**	**R (Ω)**
-0.3	-0.00192	156.25	-0.3	-2.02E-04	1.49E+03
-0.2	-0.00124	161.2903	-0.2	-9.85E-05	2.03E+03
-0,1	-5.63E-4	177.6199	-0.1	-4.51E-05	2.22E+03
0.1	7.26E-4	137.741	0.1	1.20E-04	8.33E+02
0.2	0.00157	127.3885	0.2	2.51E-04	7.97E+02
0.3	0.00244	122.9508	0.3	3.91E-04	7.67E+02
		$R_{average}$=147.2068			$R_{average}$=1.36E+03

CHAPTER 4

ALL SOLUTION PROCESSED, NANOWIRE ENHANCED UV PHOTODETECTORS

4.1 Introduction

The existence of UV radiation was first mentioned in 1801 by J. W. Ritter. He observed that a number of chemical reactions were accelerated by a radiation, which was not visible to human eye and had a wavelength shorter than the violet light. Then, in 1804, it was shown that this radiation was subject to the laws of interference similar to the visible light. At the beginning of the 19^{th} century, it was found that although visible and UV radiation have different wavelengths, they revealed the same electromagnetic properties.

It is known that the UV radiation occupies the spectral interval of 400-10 nm and it is divided into four categories, namely:

- UVA, including wavelengths between 400 and 320 nm,
- UVB, covering wavelengths from 320 to 280 nm,
- UVC, for wavelengths ranging from 280 and 200 nm,
- The far UV, for wavelengths between 200 and 10 nm.

The most important UV source is the sun. Due to the atmosphere's absorption properties, it prevents the free propagation of light with the wavelengths below 200 nm. Therefore, the UV region ranging from 200-10 nm cannot propagate except in vacuum and it is known as vacuum UV. It is usually assumed that the radiation with

wavelengths below 280 nm does not reach the Earth's surface. Therefore, UVA and UVB are responsible for the biological effects of the sun [74].

UV photodetection is especially important for the use in military and medical applications [75-77]; such as missile launch detection, flare sensing, UV calibration and monitoring, chemical and biological analysis, environmental monitoring, space research and optical communications [78]. For most of these applications, it is advantageous if the UV photodetectors are not sensitive to visible and infrared radiation. Therefore, they are classified as visible blind detectors with cutoff wavelengths in between 400-280 nm or can be named as solar blind presuming that the UVC can be blocked by the atmosphere. In addition, a suitable UV photodetector should meet the necessary requirements such as; high sensitivity in UV region, low signal to noise ratio, high selectivity and responsivity.

4.1.1 Semiconductor Photodetectors

Photoconductors, metal-semiconductor-metal photodiodes, Schottky barrier photodiodes, metal-insulator-semiconductor structures, p-n and p-i-n photodiodes, field effect and bipolar phototransistors are the examples of the semiconductor photodetectors [79].

The first fabricated semiconductor photodetectors included narrow bandgap materials such as III-V semiconducting materials and mainly silicon. However, the major drawback of these narrow bandgap semiconductors is that it is not possible to use these photodetectors directly for the detection of the UV radiation. It is because, device ageing occurs due to exposure to higher energy photons compared to the semiconductor bandgap. Another restriction of these photodetectors originates from their sensitivity to low energy radiation. As a result of this, filters should be used to block the visible and infrared radiation. In addition, the active area of the photodetector must be cooled to decrease the dark current. Nevertheless, cooling of the device leads to low sensitivity. On the other hand, wide bandgap semiconductors

can overcome many of these limitations in UV detection. For instance, they can operate at room temperature and present intrinsic visible blindness [78].

The working principle of semiconductor photodetectors involves the creation of electron-hole pairs under illumination. When the photodetector is exposed to light, the photons with energies equal to or greater than the semiconductor's bandgap excite electrons from valence to conduction band of this semiconductor. Furthermore, the holes in the valence band move from one atomic location to another by the effect of an electric field. Therefore, the separation of electron-hole pairs lead to a photocurrent, which increases with the intensity of the illumination.

Among various types of semiconductor photodetectors, photoconductors can be presented as the simplest devices, which consist of a semiconductor layer with ohmic contacts at the each end. A constant voltage is applied between the contacts and a bias current passes through the semiconductor layer. The optically active part is composed of a region between two electrodes. Under illumination, the generated photocurrent is added to the bias current, which increases the device conductivity.

4.1.2 ZnO Based UV Photodetectors

ZnO has become highly appealing due to its unique properties and various applications in optoelectronic devices. It has high chemical stability, strong radiation hardness and a large band gap (3.37 eV). In addition, ZnO can be synthesized using low cost methods.

The UV photodetection using ZnO films was first examined in the 1940s by Mollow. Nevertheless, ZnO based UV photodetectors were developed after 1980s. First studies included simple structures with unfavorable properties. After the improvement of various synthesis techniques, high performance ZnO based UV photodetectors were obtained [80].

Although thin film or bulk ZnO is sensitive to UV, single crystal nanostructures are more favorable due to their faster recovery time and higher responsivity [81-84].

Especially in nanowires, photocarrier lifetime is increased by deep-level surface trap states and transition time of the carriers decrease as a result of the reduced dimensionality of the active area [85].

The use of ZnO nanowires in UV photodetectors have been applied in two different forms. First one is the individual nanowire devices. However, these devices require intense and high cost lithographical methods, are relatively slow in response and poor in performance [86, 87]. On the other hand, nanowire network devices reveal better detector characteristics and can be fabricated with cost effective methods over large areas [88,89].

Doping of ZnO with different elements can change its bandgap and enable the fabrication of UV detectors with different cut-off wavelengths. As mentioned in the previous chapter, Al doping of ZnO has attracted much attention in terms of enhanced electrical conductivity. Therefore, ZnO:Al nanowires can provide high performance UV photodetectors.

4.1.3 Silver Nanowire Electrodes for ZnO Nanowire Based UV Photodetectors

Generally, non-transparent metal electrodes such as gold (Au) and platinum (Pt) are used in ZnO UV photodetectors [90,91]. However, these electrodes lead to a decrease in the amount of absorbed light and are deposited through high vacuum processes. Some studies have recently been carried out in order to find alternatives. To name an example, indium tin oxide (ITO) is used as back contact in ZnO nanowire based UV photodetectors [92]. Nevertheless, ITO necessitates vacuum deposition and limited indium sources increase ITO prices. These are the main obstacles for the production of a low cost and transparent ZnO UV photodetector.

Among the alternative materials for transparent and conducting contacts, random networks of Ag nanowires could be promising candidates. These transparent nanowire electrodes have already been used in organic solar cells [93]. In photodetectors, Ag nanowires could be used to transfer electrons. Hence,

recombination of photoelectrons and holes would be prevented and photoinduced electron hole pairs continue to be generated under illumination [94].

In this thesis, all solution processed ZnO-Ag nanowire heterostructured (metal-semiconductor-metal) UV photodetectors have been fabricated. Ag nanowires were used as transparent and conducting contacts. In between these nanowires, necessary channels were formed and both undoped and ZnO:Al nanowires were grown within these channels and on the surfaces of Ag nanowires by hydrothermal method. The effect of Al doping, ZnO nanowire length and in-situ annealing on the photoresponse characteristics of the fabricated photodetectors were investigated.

4.2 Experimental Details

All chemicals were purchased from Signa-Aldrich and used without further purification. Ag nanowires were synthesized according to the procedure reported by our group before [95]. In brief, in a typical synthesis, 10 ml of 0.45 M ethylene glycol (EG) solution of poly(vinylpyrrolidone) (PVP) was prepared with 7 mg of sodium chloride (NaCl, 99.5%). This solution was heated to 170°C in a two neck flask. Simultaneously, 0.12 M silver nitrate ($AgNO_3$) (99.5%) solution in a 5 ml EG was added into PVP/EG solution via an injection pump (Top-5300) at a rate of 5 ml/h. The solution was stirred throughout the process. Upon the completion of $AgNO_3$/EG addition, solution was annealed at 170°C for another 30 minutes. Following the synthesis, solution was diluted with acetone (1:5) and centrifuged twice at 7000 rpm for 20 minutes. In addition, Ag nanowires were suspended in ethanol and same centrifuging process was applied. Finally, Ag nanowires were redispersed in ethanol for further processing. Ethanolic Ag nanowire dispersion was deposited onto the glass substrates by spray coating. For this purpose, nitrogen driven air brush was used. As-coated Ag nanowires were annealed at 200°C for 30 minutes in order to decrease the contact resistance between the nanowires. Hence, Ag nanowire networks with a transmittance and sheet resistance of 80% and 5 Ω/square were obtained, respectively.

Following their deposition, transparent and conducting Ag nanowire networks were mechanically scratched using a razor blade to provide a channel for the growth of ZnO nanowires. Ag paste pads were used as the ultimate contacts for devices. Ag nanowire network deposited glass substrates were then spin coated with a 5 mM zinc acetate dihydrate ($Zn(C_2H_3O_2)_2.2H_2O$, 99.9%) solution dissolved in 1-propanol to form the seed layer for the ZnO nanowire growth. Seeded samples were then dipped into the growth solutions containing 20 mM zinc acetate dihydrate and 20 mM hexamethylenetetramine (HMTA) for undoped ZnO nanowires and 1 mM Al acetate, 19 mM zinc acetate dihydrate and 20 mM HMTA for ZnO:Al nanowires. These solutions were kept at 90°C during the growth. Photodetectors with different nanowire lengths, simply controlled by the growth duration (1-3 hours), have been fabricated to investigate the effect of nanowire length on the device performance.

4.3. Photodetector Characterization Methods

4.3.1 Scanning Electron Microscopy (SEM)

The morphology of the ZnO nanowires were analyzed by FESEM (Nova NanoSEM 430) operated at a voltage of 10 kV. Cross-sectional SEM images were obtained from cleaved edges of the substrates. Gold coating was used to provide conductivity to the glass substrates for analysis.

4.3.2 Transparency Measurements

Optical UV-Visible (UV-VIS) transmission measurements were taken using VARIAN CARY 100 BIO UV-Visible Spectrometer in normal incidence mode from bare Ag nanowires, undoped and doped ZnO nanowires grown on glass substrates within a wavelength range of 300-800 nm. Bare glass substrates have been used as reference.

4.3.3 X-Ray Diffraction Measurements

The crystal structure of the Ag and ZnO nanowires was investigated using X-Ray diffraction (XRD) analysis. A Rigaku D/Max-2000 PC diffractometer was employed, using Cu-Kα radiation (λ=1.54056 Å) and X-Ray source operating voltage of 40 kV in the 2θ range of 30-60° at a scanning rate of 2°/min.

4.3.4 Photoluminescence Measurements

To investigate the optical characteristics of ZnO nanowires, photoluminescence (PL) measurements were performed using a HORIBA Jobin Yvon PL system at an excitation wavelength of 325 nm. Measurements were conducted at room temperature.

4.3.5 Spectral Response Measurements

The spectral response measurements of the ZnO nanowire photodetectors were carried out at room temperature using a spectral response set-up schematically shown in Figure 4.1. The light was generated by a Newport Oriel Apex Monochromator Illuminator with a halogen lamp light source. The light beam was sent to a Newport Oriel 74125 Monochromator. The resulting monochromatic light within the range of wavelengths from 300 to 550 nm was projected to the ZnO nanowire photodetectors. A bias voltage of 2V was applied via a Keithley 2400 sourcemeter. The obtained photoresponse spectrum was corrected for the spectral distribution of the illumination light. The power spectrum of the light was obtained using a Newport powermeter.

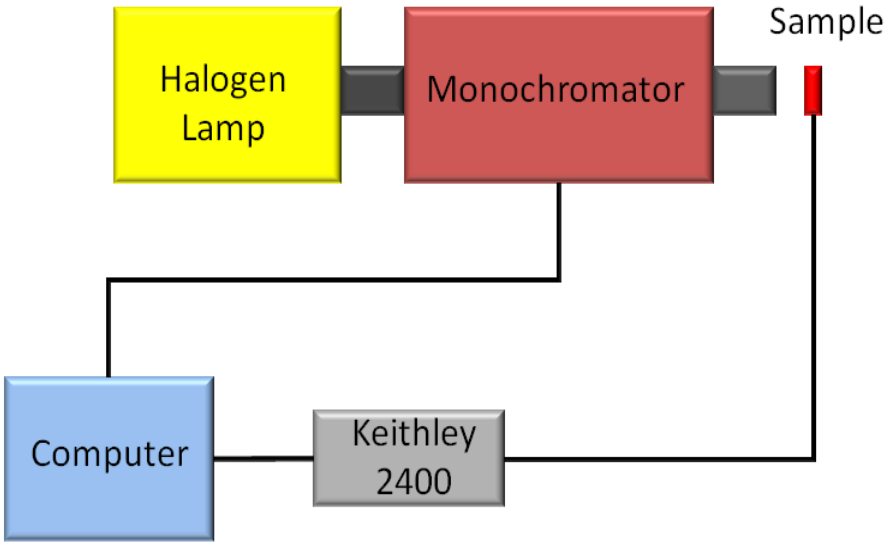

Figure 4.1 The schematic diagram of the spectral response measurement setup used in the experiments.

4.3.6 Current-Voltage Measurements

I-V measurements have been performed using a Keithley 2400 sourcemeter as the voltage source. Voltage was swept between -2 V to 2 V for all samples and the following current values were obtained using a Labview program.

4.3.7 Photocurrent Measurements

Photocurrent measurements were made under a constant DC bias of 2 V applied by a Keithley 2400 sourcemeter. Photocurrents under dark and UV illumination were recorded by switching the 8W UV lamp (Vilber Laurbat, 365nm) on and off.

4.4 Results and Discussion

The SEM images showing top and cross-sectional views of ZnO photodetectors with different nanowire lengths are shown in Figure 4.2. ZnO nanowires grown within the gap can be easily distinguished from the ones grown on and between the Ag nanowires in Figure 4.2 (a). A typical gap size of 7 μm was used for the devices. In addition, the inset of Figure 4.2 (a) shows the ZnO nanowires that were grown on a single Ag nanowire. SEM images of the ZnO nanowires kept in the growth solution for 1, 2 and 3 hours are shown in Figure 4.2 (b)-(d), respectively. As it can be seen, with an increase in the growth duration from 1 to 3 hours, the length of the ZnO nanowires changes from 700 nm to 2.2 μm, respectively.

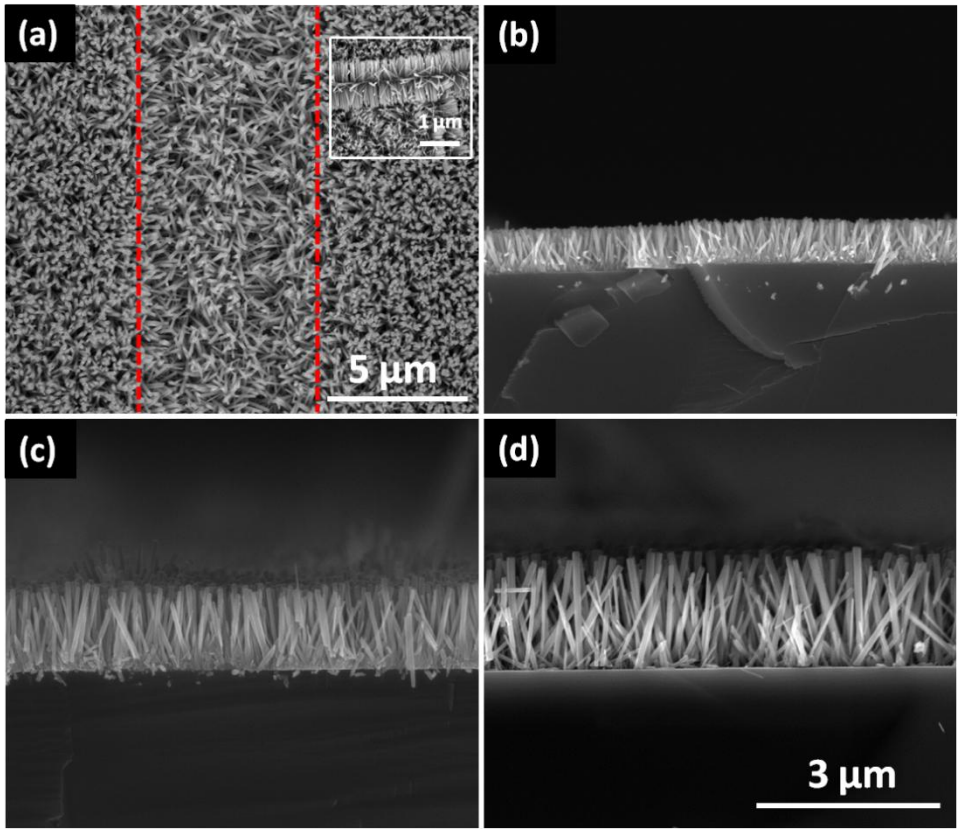

Figure 4.2 SEM images of (a) top-view of the gap region and cross-sectional view of ZnO nanowires with different lengths of (b) 0.7, (c) 1.2 and (d) 2.2 μm. Scale bars for (b), (c) and (d) parts are the same.

Moreover, as mentioned in Chapter 3, ZnO:Al nanowires had wurtzite structure and no change in hexagonal morphology was observed. When the growth duration increased from 1 to 3 hours, the length of Al doped nanowires also increased as in the case of undoped counterparts.

Since Ag nanowire network was used as the contacts instead of Pt or Au thin films, fabricated ZnO nanowire photodetectors show considerable transparency in the visible region. Visible transmittance of ZnO/Ag nanowire photodetectors are shown in Figure 4.3 (a). Transmittance of bare Ag nanowire network electrode is also provided for comparison. As it can be seen from the graph, pristine Ag nanowire networks show a visible transmittance around 80% (at 550 nm). The growth of undoped ZnO and ZnO:Al nanowires on Ag nanowire network decreases the transparency of the devices to 70% and 60%, respectively. But still, it is evident from the Figure 4.3 (b) that the fabricated ZnO nanowire photodetectors have adequate transparency in the visible range. XRD patterns of Ag and ZnO nanowires are shown in Figure 4.3 (c). All reflected peaks belong to pure Ag and ZnO (JCPDS Card No: 36-1451 and 04-0783 for ZnO and Ag, respectively). The XRD pattern of ZnO:Al nanowires was revealed in Chapter 3 and it was seen that the preferred orientation of ZnO:Al nanowires was also in the (002) direction, with no detectable Al peak.

Room temperature PL spectra of both doped and undoped ZnO nanowires are shown in Figure 4.4 (d). Undoped sample exhibited a strong peak at 378 nm, which represents the near band edge emission and a weak broad peak centered around 545 nm, which could be attributed to deep level defects in ZnO crystal structure. In addition, as it is mentioned earlier, from the PL spectrum of the ZnO:Al nanowires, the band edge transition peak was observed at 382 nm. UV peak shift due to Al doping was related with the bandgap reduction.

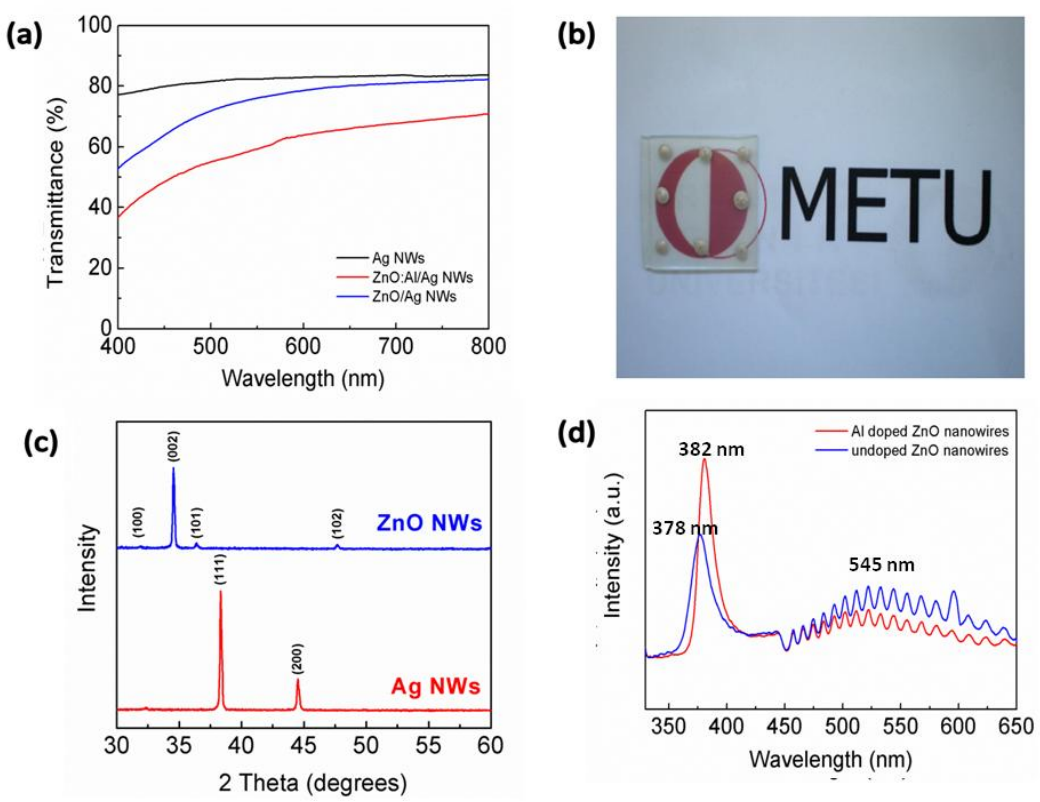

Figure 4.3 (a) Transmittance spectra of the ZnO/Ag photodetectors. (b) A photograph of transparent ZnO/Ag photodetectors fabricated on glass substrates. (c) XRD pattern of the ZnO and Ag nanowires. (d) PL spectra of both undoped and ZnO:Al nanowires at room temperature.

Schematic drawing of ZnO nanowire based photodetectors is shown in Figure 4.4 (a). Since the conductivity of Ag is higher than that of ZnO, the ZnO nanowires grown on Ag nanowires will not have a considerable effect on the photocurrent of the devices. Hence, it can be assumed that the ZnO nanowires grown within the gap between Ag nanowires determine the photocurrent of the fabricated detectors.

The photoresponse current is one of the most important characteristics of the photodetectors. It is generally defined as the difference between the photocurrent, measured under illumination and dark state. Due to large bandgap of ZnO, a high response in the UV part of the spectrum is expected. However, the precise wavelengths over which highest responsivity can be obtained must be determined.

For this purpose, spectral response measurements were made between wavelengths of 300-550 nm under a forward bias of 2V. As it is seen from the Figure 4.4 (b), a sharp cut-off responsivity was obtained around 380 nm from undoped ZnO nanowires and 385 nm from ZnO:Al nanowires, which correspond to band edge absorption of ZnO. When this result is compared to the PL measurements a slight shift in the position of the maximum peak (378 nm and 382 nm) is observed. This could be attributed to heating effect of the current, which could decrease the effective bandgap of ZnO [96]. In addition, the responsivity of the undoped and ZnO:Al nanowire UV photodetectors were measured as 0.46 A/W at 380 nm and 2.78 A/W at 385 nm, respectively. The large photocurrent can be attributed to higher number of carriers collected under illumination with Al doping in the ZnO nanowires.

It is well known that, UV photoresponse characteristics of ZnO nanowire based photodetectors are mainly determined by the adsorption and desorption of oxygen as well as water molecules [97]. It was reported that under UV illumination, the photocurrent of ZnO nanowire based photodetectors is negatively affected by the presence of water molecules in air due to the exchange mechanism of hydroxyl groups and ionic oxygen [98]. In order to prevent this, the fabricated detectors were in-situ heated to 150°C via a hot plate during measurements to ensure complete removal of water molecules from the lateral surfaces of the ZnO nanowires. This allowed the photoresponse characteristics of our UV photodetectors to get only affected by the adsorption and desorption of oxygen molecules.

The basic working mechanism of ZnO nanowire based photodetectors is schematically presented in Figure 4.4 (c) and can be explained as follows. In the dark state, oxygen molecules adsorbed on the surface of ZnO nanowires capture free electrons and depletion layer forms near the nanowire surface. Therefore, oxygen molecules turn into negatively charged ions and the total carrier concentration decreases and so does the conductivity of the ZnO nanowires. When the nanowires are subjected to UV illumination with energies larger than the bandgap of ZnO, electron and hole pairs are generated. The photogenerated holes migrate to negatively charged oxygen ions and neutralize them. These neutralized oxygen molecules desorb from the surface of ZnO nanowires. Hence, the photocurrent

increases due to released unpaired electrons until desorption and readsorption of oxygen molecules reach an equilibrium state. After turning off the UV illumination, holes and electrons recombine with each other; however, extra electrons still remain in the ZnO nanowires. These extra electrons are captured by readsorbed oxygen molecules. As a result, the conductivity of the nanowires decreases.

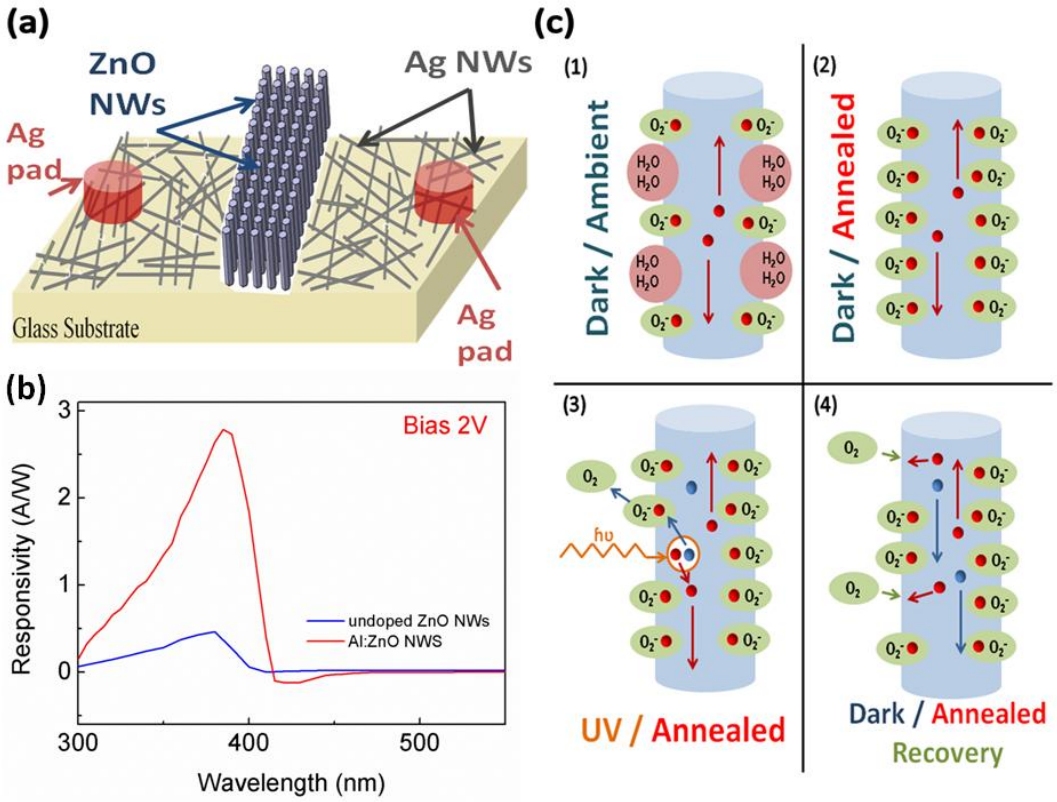

Figure 4.4 (a) ZnO/Ag nanowire UV photodetector device architecture. (b) Photoresponsivity of ZnO/Ag nanowire based photodetectors under a bias of 2V. (c) Schematic of the photoresponse process.

Representative I-V characteristics of the fabricated undoped ZnO nanowire based devices under illumination and at dark are shown in Figure 4.5 (a). Ohmic contact evidenced by the straight I-V characteristics of the device was obtained between Ag and ZnO nanowires. This can be due to the high carrier density in the ZnO nanowires

grown by hydrothermal method. At a bias of 2 V, the dark current was about 0.0486 μA and when the detector was illuminated with a 365 nm UV lamp, the current was measured to be 127.4 μA. In addition, the ratio of the photocurrent to dark current (on/off ratio) is calculated as 2600. This result is in reasonable agreement when compared to the photodetectors fabricated in a similar fashion [99].

Figure 4.5 (b) shows the UV photoresponse properties of ZnO nanowires measured at 150°C. For comparison, the photoresponse characteristics at room temperature is also provided within the same figure. As it can be seen, heated sample exhibits shorter response and recovery times and a higher photocurrent. High response and recovery times and low photocurrent of the detector at room temperature could be attributed to the effect of water molecules adsorbed on the surfaces of ZnO nanowires. Heated photodetector may also enhance the readsorption of oxygen molecules to the surface of the ZnO nanowires resulting in fast photoresponse properties. Fujita et. al. [100] revealed that the adsorption of oxygen molecules on ZnO surfaces is activated and favored at 150°C. Therefore, ZnO nanowire photodetectors heated to 150°C showed short recovery times.

In Figure 4.5 (c), photoresponse characteristics of the ZnO nanowire based photodetectors with different nanowire lengths are compared. As it is evident, increase in nanowire length enhances the photocurrent of the detectors. This result may arise from the absorption of more photons and generation of higher number of charge carriers by longer nanowires. Beyond a certain nanowire length, although the photocurrent is high, response and recovery times get longer. This can be attributed to the formation of more charge traps and scattering centers in longer nanowires. Those defects are known to adversely affect the photodetectors by increasing recombination and decreasing photoresponse [101].

In Figure 4.5 (d), photoresponse characteristics of ZnO:Al nanowire based photodetectors with different nanowire lengths are also showed. As it can be seen, compared to undoped nanowires, doped nanowire based photodetectors have higher current values, which was also revealed through photoresponse measurements. However, these detectors have slow response and recovery times. Al donor states located below the conduction band leads to an impurity band, which overlaps the

bottom of the conduction band. The increase in carrier concentration and donor states due to doping can be the reasons for the slow recovery and response times of doped nanowires.

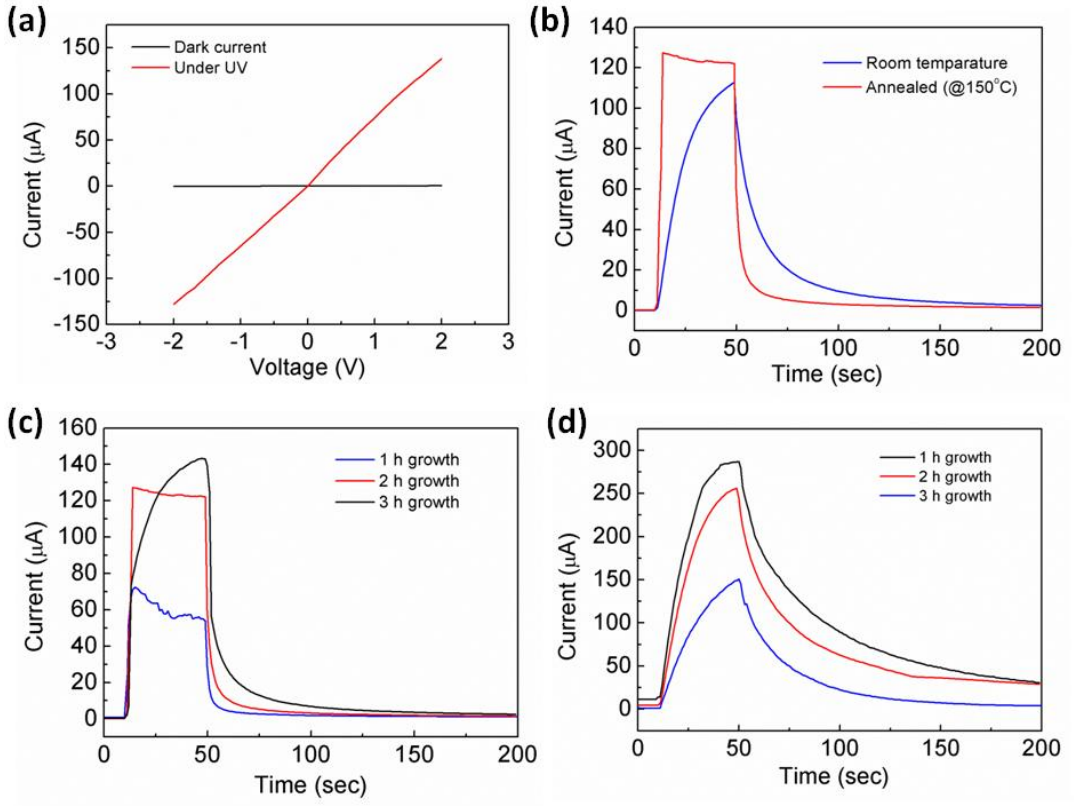

Figure 4.5 (a) I-V characteristics of a fabricated detector at dark and under illumination. Effect of (b) annealing and (c) ZnO nanowire length on the photoresponse characteristics of the detector. (d) Photoresponse characteristics of ZnO:Al nanowire photodetectors with different nanowire lengths.

Performance of the detectors was investigated in detail and the recovery times (τ) of the undoped and ZnO:Al nanowire based detectors were examined. Recovery time can be defined as the time in which the photocurrent decreases to 80% from its maximum value. Photoresponse characteristics of the devices with undoped ZnO and ZnO:Al nanowires are shown in Figure 4.6 (a) and (b), respectively. The recovery

times of the devices were calculated as 4 and 65 seconds, respectively. The devices with undoped ZnO has short recovery times, which is faster than other ZnO nanowire based photodetectors having similar device architecture [102].

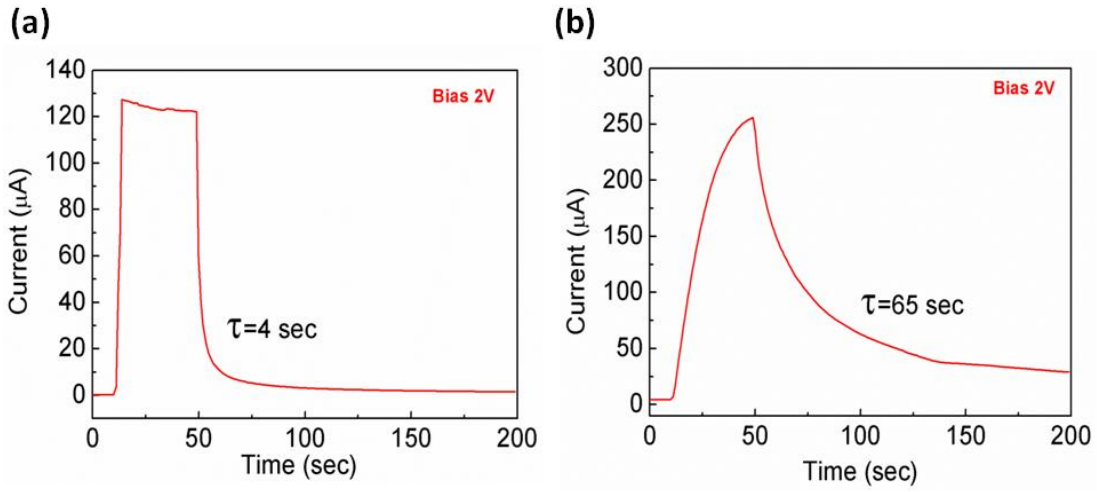

Figure 4.6 Response and recovery characteristics of (a) undoped and (b) ZnO:Al nanowires at a bias of 2V.

CHAPTER 5

CONCLUSIONS AND FUTURE RECOMMENDATIONS

5.1. Conclusions

In this thesis, synthesis and doping of ZnO nanowires by hydrothermal method were investigated. The pure and doped ZnO nanowires with transparent Ag nanowire network electrodes were utilized in all solution processed UV photodetectors.

In the first stage, the hydrothermal growth mechanism was explained and synthesized ZnO nanowires were characterized. The hydrothermal method involves the use of Zn acetate with HMTA in solution and the growth is carried out at low temperatures. This method is highly appealing due to its simplicity and low cost compared to other synthesis techniques.

In the second part, synthesis and characterization of doped ZnO nanowires using hydrothermal method was reported. The metal dopants such as, Cu, Ag and Al were used to dope ZnO nanowires to impart and then examine magnetic properties, p-type doping and enhanced conductivity, respectively. Doping procedure included the addition of Cu (II) acetate monohydrate, Ag acetate or Al acetate with different concentrations into the growth solutions. The existence of Cu, Ag and Al atoms in ZnO lattice were characterized and confirmed with various analytical methods. ZnO:Cu nanowires showed enhanced magnetic properties due to the homogeneous distribution of Cu atoms in the structure. To investigate p-type conductivity of ZnO:Ag nanowires, p-n homojunction diodes were fabricated. However, the homojunctions showed symmetric I-V curves, which means no rectification was obtained. This could be due to the dopants, which could not get activated within the

structure or to the short circuit between top and bottom contacts. In addition, p-type doping may not be stable. To analyze the effect of Al doping on ZnO nanowires, electrical measurements were carried out. Compared to the undoped ZnO nanowires, Al doped ones showed higher current values, indicating an enhancement in conductivity.

In the third part, Ag/ZnO nanowire based UV photodetectors were fabricated and characterized. The effect of nanowire length and in-situ heating were investigated. Hydrothermal and polyol methods, which are all solution based, were used for the synthesis of ZnO and Ag nanowires, respectively. Ag nanowires were utilized as electrodes, whereas undoped and ZnO:Al nanowires were used as active semiconductors. Fabricated photodetectors revealed high optical transparency in the visible region. Moreover, detectors heated to 150°C, showed shorter response and recovery times and increased photocurrent compared to the ones measured at room temperature. Photodetectors fabricated with longer nanowires were found to have larger photocurrent. However, beyond a certain nanowire length, the photoresponse of the device was deteriorated. In addition, ZnO:Al nanowire based photodetectors have higher photocurrent values. Nevertheless, these detectors have slow response and recovery times due to increase in carrier concentration. Therefore, these slow photoresponse times obtained from ZnO:Al nanowires hinders the fabrication of fast UV photodetectors. On the other hand, ZnO:Al nanowires can be convenient for low voltage operations. The photodetectors with 1.2 μm long undoped ZnO nanowires exhibited a recovery time and on/off ratio of 4 seconds and 2600, respectively. Our results simply reveal the potential of nanowire-nanowire heterojunctions to be used in various other photonic devices.

5.2. Future Recommendations

In this thesis, hydrothermal growth and doping of ZnO nanowires were investigated. To dope the nanowires different metals were tried to be added into the structure. The introduction of these dopants into the ZnO structure can be improved by controlled annealing, which can lead to better activation of the metal atoms. The electrical

measurements such as conductivity, field effect mobility can be done on an individual nanowire prepared by lithographic techniques. This is because Hall-Effect measurements are almost impossible to apply to the nanowire structure. Cu doping can also be investigated in detail with different dopant concentrations to examine the magnetic properties of ZnO:Cu nanowires. In addition, Rietveld refinement can be carried out to obtain detailed quantitative analysis of ZnO lattice upon doping.

On the other hand, undoped and ZnO:Al nanowires were grown vertically in between the gap of Ag nanowire network electrodes to fabricate UV photodetectors and the electrical conduction was provided through the gap between the Ag electrodes and ZnO nanowires. The photoresponse characteristics of the detectors can be improved by oxygen plasma treatment and the response time can be further decreased using ZnO nanowires grown vertically between top and bottom electrodes.

REFERENCES

[1] Baruah S., Dutta J., 2009, "Hydrothermal growth of ZnO nanostructures", Science and Technology of Advanced Materials, 10, 013001.

[2] Yang P., Yan H., Mao S., Russo R., Johnson J., Saykally R., Morris N., Pham J., He R., Choi H. J., 2002, "Controlled growth of ZnO nanowires and their optical properties," Advanced Functional Matters, 12, 323.

[3] Tornow J., Schwarzburg K., 2007, "Transient Electrical Response of Dye-Sensitized ZnO Nanorod Solar Cells", Journal of Physical Chemistry C, 111, 8692.

[4] Wang Z. L., Song J., 2006, "Piezoelectric Nanogenerators Based on Zinc Oxide Nanowire Arrays", Science, 312, 242.

[5] Unalan H. E., Zhang Y., Hiralal P., Dalal S., Chu D. P., Eda G., Teo K. B. K., Chhowalla M., Milne W. I., Amaratunga G. A. J., 2009, "Zinc oxide nanowire networks for macroelectronic devices", Applied Physics Letters, 94, 163501.

[6] Zhu Z., Zhang L., Howe J. Y., Liao Y., Speidel J. T., Smith S., Fong H., 2009, "Aligned electrospun ZnO nanofibers for simple and sensitive ultraviolet nanosensors", Chemical Communications, 2568.

[7] Litton C. W., Reynolds D. C., Collins T. C., 2011, "Zinc Oxide Materials for Electronic and Optoelectronic Device Applications", John Wiley & Sons, London, UK, 1st Edition.

[8] Ozgur U., Alivov Y. I., Liu C., Teke A., Reshchikov M. A., Dogan S., Avrutin V., Cho S. J., Morkoc H., 2005, "A Comprehensive Review of ZnO Materials and Devices", Journal of Applied Physics, 98, 041301.

[9] Klingshirn C., 2007, "ZnO: From basics towards applications", Physica Status Solidi (b), 244, 3027.

[10] Sun X. W., Kwok H. S., 1999, "Optical properties of epitaxially grown zinc oxide films on sapphire by pulsed laser deposition", Journal of Applied Physics, 86, 408.

[11] Bhushan B., 2007, “Springer Handbook of Nanotechnology,” Springer, 2nd Edition.

[12] Chang Y. K., Hong F. C. N., 2009, “The fabrication of ZnO nanowires field-effect transistors combining dielectrophoresis and hot-pressing”, Nanotechnology, 20, 235202.

[13] Cha S. N., Jang J. E., Choi Y., Amaratunga G. A. J., 2006, “High performance ZnO nanowire field effect transistor using self-aligned nanogap gate electrodes”, Applied Physics Letters, 89, 263102.

[14] Lupan O., Pauporte T., Viana B., 2010, “Low-Voltage UV-Electroluminescence from ZnO-Nanowire Array/p-GaN Light-Emitting Diodes”, Advanced Materials, 22, 3298.

[15] Law J. B. K., Thong J. T. L., 2008, “Improving the NH3 gas sensitivity of ZnO nanowire sensors by reducing the carrier concentration”, Nanotechnology, 19, 205502.

[16] Soci C., Zhang A., Xiang B., Dayeh S. A., Aplin D. P. R., Park J., Bao X. Y., Lo Y. H., Wang D., 2007, “ZnO Nanowire UV Photodetectors with High Internal Gain”, Nano Letters, 7, 1003.

[17] Law M., Greene L., Johnson J. C., Saykally R., Yang P., 2005, “Nanowire dye-sensitized solar cells”, Nature Materials, 4, 455.

[18] Wang X., Sun X. Y., Fairchild M., Hersee S. D., 2006, “Fabrication of GaN nanowire arrays by confined epitaxy”, Applied Physics Letters, 89, 233115.

[19] Chen M. T., Lu M. P., Wu Y. J., Song J., Lee C. Y., Lu M. Y., Chang Y. C., Chou L. J., Wang Z. L., Chen L. J., 2010, “Near UV LEDs Made with in Situ Doped p-n Homojunction ZnO Nanowire Arrays”, Nano Letters, 10, 4387.

[20] Yang Y., Sun X. W., Tay B. K., You G. F., Tan S. T., Teo K. L., 2008, “A p-n homojunction ZnO nanorod light-emitting diode formed by As ion implantation”, Applied Physics Letters, 93, 253107.

[21] Zhang J. Y., Li P. J., Sun H., Shen X., Deng T. S., Zhu K. T., Zhang Q. F., Wu J. L., 2008, “Ultraviolet electroluminescence from controlled arsenic-doped ZnO nanowire homojunctions”, Applied Physics Letters, 93, 021116.

[22] Fang X., Li J., Zhao D., Shen D., Li B., Wang X., 2009, “Phosphorus-Doped p-Type ZnO Nanorods and ZnO Nanorod p-n Homojunction LED Fabricated by Hydrothermal Method”, Journal of Physical Chemistry C, 113, 21208.

[23] Mitra P., Chatterjee A. P., Maiti H. S., 1998, "ZnO thin film sensor" Materials Letters, 35, 33.

[24] Kind H., Yan H., Messer B., Law M., Yang P., 2002, "Nanowire Ultraviolet Photodetectors and Optical Switches", Advanced Materials, 14, 158.

[25] Baxter J. B., Aydil E. S., 2005, "Nanowire-based dye-sensitized solar cells", Applied Physics Letters, 86, 053114.

[26] Choe M., Hong W. K., Park W., Yoon J., Jo G., Kwon T., Welland M. E., Lee T., 2012, "UV photoconductivity characteristics of ZnO nanowire field effect transistor treated by proton irradiation", Thin Solid Films, 520, 3624.

[27] Qurashi A., Tabet N., Faiz M., Yamzaki T., 2009, "Ultra-fast Microwave Synthesis of ZnO Nanowires and their Dynamic Response Toward Hydrogen Gas", Nanoscale Research Letters, 4, 948.

[28] Sun X. W., Huang J. Z., Wang J. X., Xu Z., 2008, "A ZnO Nanorod Inorganic/Organic Heterostructure Light-Emitting Diode Emitting at 342 nm", Nano Letters, 8, 1219.

[29] Chen C. H., Chang S. J., Chang S. P., Li M. J., Chen I. C., Hsueh T. J., Hsu C. L., 2009, "Novel fabrication of UV photodetector based on ZnO nanowire/p-GaN heterojunction", Chemical Physics Letters, 476, 69.

[30] Li Y., Meng G. W., Zhang L. D., Phillipp F., 2000, "Ordered semiconductor ZnO nanowire arrays and their photoluminescence properties", Applied Physics Letters, 76, 2011.

[31] Huang M. H., Wu Y. Y., Feick H., Tran N., Weber E., Yang P., 2001, "Catalytic Growth of Zinc Oxide Nanowires by Vapor Transport", Advanced Materials, 13, 113.

[32] Wang Z. L., 2004, "Zinc oxide nanostructures: growth, properties and applications", Journal of Physics: Condensed Matter, 16, R829.

[33] Lyu S. C., Zhang Y., Lee C. J., Ruh H., Lee H. J., 2003, "Low-Temperature Growth of ZnO Nanowire Array by a Simple Physical Vapor-Deposition Method", Chemistry of Materials , 15, 3294.

[34] Chang P. C., Fan Z., Wang D., Tseng W. Y., Chiou W. A., Hong J., Lu J. G., 2004, "ZnO Nanowires Synthesized by Vapor Trapping CVD Method", Chemistry of Materials, 16, 5133.

[35] Lee D. H., Son K., Park W. I., 2010, “Patterned synthesis of laterally oriented ultrafine ZnO nanowires by controlled metalorganic chemical vapour deposition”, Journal of Physics D: Applied Physics, 43, 245402.

[36] Elias J., Tena-Zaera R., Le´vy-Cle´ment C., 2008, “Electrochemical deposition of ZnO nanowire arrays with tailored dimensions”, Journal of Electroanalytical Chemistry, 62, 171.

[37] Xu S., Wang Z. L., 2011, “One-Dimensional ZnO Nanostructures: Solution Growth and Functional Properties”, Nano Research, 4, 1013.

[38] Vergés M. A., Mifsud A., Serna C. J., 1990, “Formation of rod-like zinc oxide microcrystals in homogeneous solutions” Journal of the Chemical Society, Faraday Transactions, 86, 959.

[39] Vayssieres L., 2003, “Growth of Arrayed Nanorods and Nanowires of ZnO from Aqueous Solutions” Advanced Materials, 15, 464.

[40] Greene L.E., Law M., Tan D.H., Montano M., Goldberger J., Somorjai G., Yang P., 2005, “General route to vertical ZnO nanowire arrays using textured ZnO seeds”, Nano Letters, 5, 1231.

[41] Yuan G. D., Zhang W. J., Jie J. S., Fan X., Zapien J. A., Leung Y. H., Luo L. B., Wang P. F., Lee C. S., Lee S. T., 2008, “p-Type ZnO Nanowire Arrays”, Nano Letters, 8, 2591.

[42] Janotti A., Walle C. G. V., 2007, “Native point defects in ZnO”, Physical Review B, 76, 165202.

[43] Sun X. W., Yang Y., 2012, “ZnO Nanostructures and Their Applications”, Pan Stanford Publishing Pte. Ltd.

[44] Gayen R. N., Rajaram A., Bhar R., Pal A. K., 2010, “Ni-doped vertically aligned zinc oxide nanorods prepared by hybrid wet chemical route”, Thin Solid Films, 518, 1627.

[45] Xu H. J., Zhu H. C., Shan X. D., Liu Y. X., Gao J. Y., Zhang X. Z., Zhang J. M., Wang P. W., Hou Y. M., Yu D. P., 2010, “Effects of annealing on the ferromagnetism and photoluminescence of Cu-doped ZnO nanowires”, Journal of Physics: Condenced Matter, 22, 016002.

[46] Wang G., Chu S., Zhan N., Zhou H., Liu J., 2011, “Synthesis and characterization of Ag-doped p-type ZnO nanowires”, Applied Physics A, 103, 951.

[47] Chen J. T., Wang J., Zhuo R. F., Yan D., Feng J. J., Zhang F., Yan P.X., 2009, "The effect of Al doping on the morphology and optical property of ZnO nanostructures prepared by hydrothermal process", Applied Surface Science, 255, 3959.

[48] Zhou M., Zhu H., Jiao Y., Rao Y., Hark S., Liu Y., Peng L., Li Q., 2009, "Optical and Electrical Properties of Ga-Doped ZnO Nanowire Arrays on Conducting Substrates", Journal of Physical Chemistry C, 113, 8945.

[49] Xu L., Su Y., Chen Y., Xiao H., Zhu L., Zhou Q., Li S., 2006, "Synthesis and Characterization of Indium-Doped ZnO Nanowires with Periodical Single-Twin Structures", Journal of Physical Chemistry B, 110, 6637.

[50] Dai Z., Nurbawono A., Zhang A., Zhou M., Feng Y. P., Ho G. W., Zhang C., 2011, "C-doped ZnO nanowires: Electronic structures, magnetic properties, and a possible spintronic device", Journal of Chemical Physics, 134, 104706.

[51] Gao J., Zhang X., Sun Y., Zhao Q., Yu D., 2010, "Compensation mechanism in N-doped ZnO nanowires", Nanotechnology, 21, 245703.

[52] Cao B. Q., Lorenz M., Rahm A., Wenckstern H., Czekalla C., Lenzner J., Benndorf G., Grundmann M., 2007, "Phosphorus acceptor doped ZnO nanowires prepared by pulsed-laser deposition", Nanotechnology, 18, 455707.

[53] Cui J. B., Soo Y. C., Chen T. P., 2008, "Low-Temperature Growth and Characterization of Cl-Doped ZnO Nanowire Arrays", Journal of Physical Chemistry C, 112, 4475.

[54] Li H., Huang Y., Zhang Q., Qiao Y., Gu Y., Liu J., Zhang Y., 2011, "Facile synthesis of highly uniform Mn/Co-codoped ZnO nanowires: Optical, electrical, and magnetic properties", Nanoscale, 3, 654.

[55] Zou C. W., Shao L. X., Guo L. P., Fu D. J., Kang T. W., 2011, "Ferromagnetism and ferroelectric properties of (Mn, Li) co-doped ZnO nanorods arrays deposited by electrodeposition", Journal of Crystal Growth, 331, 44.

[56] Das S. N., Choi J. H., Kar J. P., Lee T. I., Myoung J. M., 2010, "Fabrication of p-type ZnO nanowires based heterojunction diode", Materials Chemistry and Physics, 121, 472.

[57] Park C. H., Zhang S. B., Wei S. H., 2002, "Origin of p-type doping difficulty in ZnO: The impurity perspective", Physical Review B, 66, 073202.

[58] Liu C., Yun F., Morkoc H., 2005, “Ferromagnetism of ZnO and GaN: A Review”, Journal of Material Science: Materials in Electronics, 16, 555.

[59] Gao D., Xu Y., Zhang Z., Gao H., Xue D., 2009, “Room temperature ferromagnetism of Cu doped ZnO nanowire arrays”, Journal of Applied Physics, 105, 063903.

[60] Xu C., Yang K., Huang L., Wang H., 2009, “Cu-doping induced ferromagnetism in ZnO nanowires”, Journal of Chemical Physics, 130, 124711.

[61] Fan J., Freer R., 1995, “The roles played by Ag and Al dopants in controlling the electrical properties of ZnO varistors”, Journal of Applied Physics, 77, 4795.

[62] Song Y. W., Kim K., Ahn J. P., Jang G. E., Lee S. Y., 2009, “Physically processed Ag-doped ZnO nanowires for all-ZnO p–n diodes”, Nanotechnology, 20, 275606.

[63] Lin D., Wu H., Pan W., 2007, “Photoswitches and Memories Assembled by Electrospinning Aluminum-Doped Zinc Oxide Single Nanowires”, Advanced Materials, 19, 3968.

[64] Yang C., Barrelet C. J., Capasso F., Lieber C. M., 2006, “Single p-Type/Intrinsic/n-Type Silicon Nanowires as Nanoscale Avalanche Photodetectors”, Nanoletters, 6, 2929.

[65] Li Y. Q., Zapien J. A., Shan Y. Y., Liu Y. K., Lee S. T., 2006, “Manganese doping and optical properties of ZnS nanoribbons by postannealing”, Applied Physics Letters, 88, 013115.

[66] Ronning C., Gao P. X., Ding Y., Wang Z. L., Schwen D., 2004, “Manganese-doped ZnO nanobelts for spintronics”, Applied Physics Letters, 84, 783.

[67] Hsin C. L., He J. H., Lee C. Y., Wu W. W., Yeh P. H., Chen L. J., Wang Z. L., 2007, “Lateral Self-Aligned p-Type In2O3 Nanowire Arrays Epitaxially Grown on Si Substrates”, Nano Letters, 7, 1799.

[68] Duan L., Lin B., Zhang W., Zhong S., Fu Z., 2006, “Enhancement of ultraviolet emissions from ZnO films by Ag doping”, Applied Physics Letters, 88, 232110.

[69] Li Y., Zhao X., Fan W., 2011, “Structural, Electronic, and Optical Properties of Ag-Doped ZnO Nanowires: First Principles Study”, Journal of Physical Chemistry C, 115, 3552.

[70] Chen R., Zou C., Bian J., Sandhu A., Gao W., 2011, "Microstructure and optical properties of Ag-doped ZnO nanostructures prepared by a wet oxidation doping process", Nanotechnology, 22, 105706.

[71] Dhara S., Giri P. K., 2012, "Stable p-type conductivity and enhanced photoconductivity from nitrogen-doped annealed ZnO thin film", Thin Solid Films, 520, 5000.

[72] Baek S. H., Noh B. Y., Park I. K., Kim J. K., 2012, "Fabrication and characterization of silicon wire solar cells having ZnO nanorod antireflection coating on Al-doped ZnO seed layer", Nanoscale Research Letters, 7, 29.

[73] Rusu G. G., Râmbu A. P., Buta V. E., Dobromir M., Luca D., Rusu M., 2010, "Structural and optical characterization of Al-doped ZnO films prepared by thermal oxidation of evaporated Zn/Al multilayered films", Materials Chemistry and Physics, 123, 314.

[74] D. Decoster, J. Harari, 2009, "Optoelectronic Sensors", John Wiley & Sons, London, USA, 1st Edition.

[75] Zhai T., Fang X., Liao M., Xu X., Zeng H., Yoshio B., Golberg D., 2009, "A Comprehensive Review of One-Dimensional Metal-Oxide Nanostructure Photodetectors", Sensors, 9, 6504.

[76] Zhai T., Li L., Wang X., Fang X., Bando Y., Golberg D., 2010, "Recent Developments in One-Dimensional Inorganic Nanostructures for Photodetectors", Advanced Functional Materials, 20, 4233.

[77] Razeghi M., Rogalski A., 1996, "Semiconductor ultraviolet detectors", Journal of Applied Physics, 79, 7433.

[78] Monroy E., Omnes F., Calle F., 2003, "Wide-bandgap semiconductor ultraviolet photodetectors", Semiconductor Science and Technology, 18, R33.

[79] Sze S. M., Ng K. K., 2006, "Physics of Semiconductor Devices", John Wiley & Sons, London, USA, 3rd Edition.

[80] Liu K., Sakurai M., Aono M., 2010, "ZnO Based Ultraviolet Photodetectors," Sensors, 10, 8604.

[81] Soci C., Zhang A., Xiang B., Dayeh S. A., Aplin D. P. R., Park J., Bao X. Y., Lo Y. H., Wang D., 2007, "ZnO Nanowire UV Photodetectors with High Internal Gain", Nano Letters, 7, 1003.

[82] Das S. N., Moon K. J., Kar J. P., Choi J. H., Xiong J., Lee T., Myoung J. M., 2010, "ZnO single nanowire-based UV detectors", Applied Physics Letters, 97, 022103.

[83] Jin Y., Wang J., Sun B., Blakesley J. C., Greenham N. C., 2008, "Solution-Processed Ultraviolet Photodetectors Based on Colloidal ZnO Nanoparticles", Nano Letters, 8, 1649.

[84] Ghosh T., Basak D., 2010, "Highly efficient ultraviolet photodetection in nanocolumnar RF sputtered ZnO films: a comparison between sputtered, sol–gel and aqueous chemically grown nanostructures", Nanotechnology, 21, 375202.

[85] Chang S. P., Lu C. Y., Chang S. J., Chiou Y. Z., Hsueh T. J., Hsu C. L., 2011, "Electrical and Optical Characteristics of UV Photodetector With Interlaced ZnO Nanowires", IEEE Journal of Selected Topics in Quantum Electronics, 17, 990.

[86] Li Q. H., Wan Q., Liang Y. X., Wang T. H., 2004, "Electronic transport through individual ZnO nanowires", Applied Physics Letters, 84, 4556.

[87] Lupan O., Chai G., Chow L., Emelchenko G. A., Heinrich H., Ursaki V. V., Gruzintsev A. N., Tiginyanu I. M., Redkin A. N., 2010, "Ultraviolet photoconductive sensor based on single ZnO nanowire", Physica Status Solidi A, 207, 1735.

[88] Yan C., Singh N., Cai H., Gan C. L., Lee P. S., 2010, "Network-Enhanced Photoresponse Time of Ge Nanowire Photodetectors", ACS Applied Materials&Interfaces, 2, 1794.

[89] Yan C., Singh N., Lee P. L., 2010, "Wide-bandgap Zn2GeO4 nanowire networks as efficient ultraviolet photodetectors with fast response and recovery time", Applied Physics Letters, 96, 053108.

[90] Hasan K. U., Alvi N. H., Lu J., Nur O., Willander M., 2011, "Single nanowire-based UV photodetectors for fast switching", Nanoscale Research Letters, 6, 348.

[91] Hu Y., Zhou J., Yeh P. H., Li Z., Wei T. Y., Wang Z. L., 2010, "Supersensitive, Fast-Response Nanowire Sensors by Using Schottky Contacts", Advanced Materials, 22, 3327.

[92] Peng S. M., Su Y. K., Ji L. W., Young S. J., Tsai C. N., Hong J. H., Chen Z. S., Wu C. Z., 2011, "Transparent ZnO Nanowire-Network Ultraviolet Photosensor", IEEE Transactions on Electron Devices, 58, 2036.

[93] Lee J. Y., Connor S. T., Cui Y., Peumans P., 2008, "Solution-Processed Metal Nanowire Mesh Transparent Electrodes", Nano Letters, 8, 689.

[94] Gu C., Cheng C., Huang H., Wong T., Wang N., Zhang T. Y., 2009, "Growth and Photocatalytic Activity of Dendrite-like ZnO@Ag Heterostructure Nanocrystals", Crystal Growth&Design, 9, 3278.

[95] Coskun S., Aksoy B., Unalan H. E., 2011, "Polyol Synthesis of Silver Nanowires: An Extensive Parametric Study", Crystal Growth&Design, 11, 4963.

[96] Zhou H., Fang G. J., Liu N., Zhao X. Z., 2011, "Effects of thermal annealing on the performance of Al/ZnO nanorods/Pt structure ultraviolet photodetector", Materials Science and Engineering B, 176, 740.

[97] Li Y., Valle F. D., Simonnet M., Yamada I., Delaunay J. J., 2009, "Competitive surface effects of oxygen and water on UV photoresponse of ZnO nanowires", Applied Physics Letters, 94, 023110.

[98] Ahn S. E., H. J., Kim K., Kim G. T., Bae C. H., Park S. M., Kim Y. K., Ha J. S., 2007, "Origin of the slow photoresponse in an individual sol-gel synthesized ZnO nanowire", Applied Physics Letters, 90, 153106.

[99] Jung B. O., Kim D. C., Kong B. H., Kim D. W., Cho H. K., 2011, "Fully transparent vertically aligned ZnO nanostructure-based ultraviolet photodetectors with high responsivity", Sensors and Actuators B, 160, 740.

[100] Fujita Y., Kwan T., 1959, "Photoresponses For The Oxygen Adsorped on Zinc Oxide Powder", Journal of the Research Institute for Catalysis Hokkaido University, 7, 24.

[101] Cao Y., He J. H., Zhu J. L., Sun J. L., 2011, "Fabrication of carbon nanotube/silicon nanowire array heterojunctions and their silicon nanowire length dependent photoresponses", Chemical Physics Letters, 501, 461.

[102] Su Y. K., Peng S. M., Ji L. W., Wu C. Z., Cheng W. B., Liu C. H., 2010, "Ultraviolet ZnO Nanorod Photosensors", Langmuir, 26, 603.